HYDRAULIC PROPERTIES OF PHU PHAN AND SAO KHUA SANDSTONES UNDER HIGH CONFINING PRESSURE

Sawarin Champanoi

A Thesis Submitted in Partial Fulfillment of the Requirements for the Degree of Master of Engineering in Civil, Transportation and Geo-resources Engineering

Suranaree University of Technology

Academic Year 2018

สมบัติเชิงชลศาสตร์ของหินทรายภูพานและหินทรายเสาขัวภายใต้ความดันล้อมรอบสูง

นางสาวสวรินทร์ จำปาน้อย

มหาวิทยาลัยเทคโนโลยีสุรนารี

วิทยานิพนธ์นี้เป็นส่วนหนึ่งของการศึกษาตามหลักสูตรปริญญาวิศวกรรมศาสตรมหาบัณฑิต

สาขาวิชาวิศวกรรมโยธา ขนส่ง และทรัพยากรธรณี

มหาวิทยาลัยเทคโนโลยีสุรนารี

ปีการศึกษา 2561

HYDRAULIC PROPERTIES OF PHU PHAN AND SAO KHUA SANDSTONE UNDER HIGH CONFINING PRESSURE

Suranaree University of Technology has approved this thesis submitted in partial fulfillment of the requirements for a Master's Degree.

Thesis Examining Committee

(Asst. Prof. Dr. Akkhapun Wannakomol)
Chairperson

(Asst. Prof. Dr. Decho Phueakphum)
Member (Thesis Advisor)

(Assoc. Prof. Dr. Pornkasem Jongpradist)
Member

(Prof. Dr. Santi Meansiri)
Vice Rector for Academic Affairs
and Internationalization

(Assoc. Prof. Flt. Lt. Dr. Kontorn Chamniprasart)
Dean of Institute of Engineering

มหาวิทยาลัยเทคโนโลยีสุรนารี

สวรินทร์ จำปาน้อย : สมบัติเชิงชลศาสตร์ของหินทรายภูพานและหินทรายเสาขัวภายใต้ความดันล้อมรอบสูง (HYDRAULIC PROPERTIES OF PHU PHAN AND SAO KHUA SANDSTONES UNDER HIGH CONFINING PRESSURE) อาจารย์ที่ปรึกษา : ผู้ช่วยศาสตราจารย์ ดร.เดโช เผือกภูมิ, 84 หน้า.

วัตถุประสงค์ของงานวิจัยนี้คือ เพื่อศึกษาผลกระทบของความดันล้อมรอบในระดับสูงต่อค่าความซึมผ่านและค่าความพรุนของหมวดหินภูพานและเสาขัว ด้วยการทดสอบการอัดน้ำภายใต้แรงดันแบบคงที่ โดยหินทรายหมวดภูพานเป็นหินทรายเนื้อละเอียดประกอบด้วย แร่ควอตซ์ 80 เปอร์เซ็นต์ แร่เฟลด์สปาร์ 2.5 เปอร์เซ็นต์ เศษหิน 5.5 เปอร์เซ็นต์ แร่ไมกา 1.5 เปอร์เซ็นต์ และส่วนประกอบอื่น 10.5 เปอร์เซ็นต์ ส่วนหินทรายหมวดเสาขัวนั้นเป็นหินทรายเนื้อละเอียดประกอบด้วย แร่ควอตซ์ 58 เปอร์เซ็นต์ แร่เฟลด์สปาร์ 5.5 เปอร์เซ็นต์ เศษหิน 7.5 เปอร์เซ็นต์ แร่ไมกา 3 เปอร์เซ็นต์ และส่วนประกอบอื่น 26 เปอร์เซ็นต์ โดยความซึมผ่านของตัวอย่างหินทรายเสาขัวมีค่าน้อยกว่าตัวอย่างหินทรายภูพาน ซึ่งความซึมผ่านมีค่าลดลงเมื่อความเค้นล้อมรอบสูงขึ้น ค่าความซึมผ่านในทิศทางขนานกับแนวการวางตัวของชั้นหินมีค่าสูงกว่าในทิศทางตั้งฉาก ซึ่งความพรุนของหินทรายชุดภูพานสูงกว่าหินทรายชุดเสาขัวโดยเฉพาะอย่างยิ่งในสภาวะความเค้นล้อมรอบสูง ซึ่งมีค่าผันแปรจาก 4.5 ถึง 7.3 เปอร์เซ็นต์ สำหรับหินทรายชุดภูพานและมีค่าผันแปรจาก 1.9 ถึง 4.3 เปอร์เซ็นต์ สำหรับหินทรายชุดเสาขัว สัมประสิทธิ์ก้อนจะถูกนำมาคำนวณหาความสามารถที่อัดตัวได้ของชั้นหิน ผลที่ได้สามารถนำไปใช้ประเมินสัมประสิทธิ์ของการกักเก็บของชั้นหินทรายทั้งสองหมวด ผลระบุว่าค่าสัมประสิทธิ์การกักเก็บมีค่าเพิ่มขึ้นเมื่อค่าความพรุนเพิ่มขึ้น และค่าสัมประสิทธิ์การกักเก็บมีแนวโน้มลดลงตามความลึกที่เพิ่มขึ้น

มหาวิทยาลัยเทคโนโลยีสุรนารี

สาขาวิชา เทคโนโลยีธรณี ลายมือชื่อนักศึกษา สวรินทร์ จำปาน้อย

ปีการศึกษา 2561 ลายมือชื่ออาจารย์ที่ปรึกษา

SAWARIN CHAMPANOI : HYDRAULIC PROPERTIES OF PHU PHAN AND SAO KHUA SANDSTONES UNDER HIGH CONFINING PRESSURE. THESIS ADVISOR : ASST. PROF. DECHO PHUEAKPHUM, Ph.D., 84 PP.

CONFINING PRESSURE/PERMEABILITY/POROSITY/STORATIVITY

The objective of this study is to experimentally determine the permeability and effective porosity of Phu Phan and Sao Khua formations under high confining pressures. Constant head flow test has been performed on this study. Phu Phan sandstone is fine-grained comprising 80% quartz, 2.5% feldspar, 5.5% rock fragment, 1.5% mica and 10.5% other. Sao Khua sandstone is very fine-grained comprising 58% quartz, 5.5% feldspar, 7.5% rock fragment, 3% mica and 26% other. The permeability of Sao Khua sandstone is lower than that of Phu Phan sandstone. It decreases with increasing confining pressures. The permeability with flow direction parallel to the bedding planes are always greater than those normal to the bedding planes. The effective porosity of Phu Phan sandstone is higher than that of Sao Khua sandstone, particularly under high confining pressures. They range from 4.5% to 7.3% for Phu Phan sandstone and 1.9% to 4.3% for Sao Khua sandstone. The bulk modulus is used to calculated formation compressibility in order to determine the aquifer storativity. The findings can be useful for a conservative prediction the storativity of these two sandstone formations. The results show that the storativity increase when the effective porosity increase and they are decreased with increasing of depths.

School of Geotechnology Student's Signature สวรินทร์ จำปานอย

Academic Year 2018 Advisor's Signature

ACKNOWLEDGMENTS

I wish to acknowledge the funding support from Suranaree University of Technology (SUT).

I would like to express my sincere thanks to Prof. Dr. Kittitep Fuenkajorn for his valuable guidance and efficient supervision. I appreciate his strong support, encouragement, suggestions and comments during the research period. I also would like to express my gratitude to Asst. Prof. Dr. Decho Phueakphum and Dr. Prachya Tepnarong for their constructive advice, valuable suggestions and comments on my research works as thesis committee members. Grateful thanks are given to all staffs of Geomechanics Research Unit, Institute of Engineering who supported my work.

Finally, I would like to thank beloved parents for their love, support and encouragement.

Sawarin Champanoi

มหาวิทยาลัยเทคโนโลยีสุรนารี

TABLE OF CONTENTS

Page

ABSTRACT (THAI) I

ABSTRACT (ENGLISH) II

ACKNOWLEDGEMENTS III

TABLE OF CONTENTS IV

LIST OF TABLES VIII

LIST OF FIGURES X

SYMBOLS AND ABBREVIATIONS XV

CHAPTER

I INTRODUCTION 1

1.1 Background and rationale 1

1.2 Research objectives 3

1.3 Research methodology 3

1.3.1 Literature review 3

1.3.2 Sample collection and preparation 5

1.3.3 Constant head flow test 5

1.3.4 Petrographic analysis of thin sections 5

1.3.5 Applications 6

1.3.6 Discussions and conclusion 6

1.3.7 Thesis writing 6

TABLE OF CONTENTS (Continued)

Page

1.4 Scope and limitations 6

1.5 Thesis contents 7

II LITERATURE REVIEW 8

2.1 Introduction 8

2.2 Stratigraphy of northeast Thailand 8

2.2.1 Sao Khua Formation descriptions 10

2.2.1.1 Lithology 10

2.2.1.2 Petrography 11

2.2.1.3 Detrital Mineralogy 11

2.2.1.4 Stratigraphic Relationships and Thickness..12

2.2.2 Phu Phan Formation descriptions 12

2.2.2.1 Lithology 12

2.2.2.2 Petrography 13

2.2.2.3 Detrital Mineralogy 13

2.2.2.4 Stratigraphic Relationships and Thickness..14

2.3 Potential of groundwater in the northeastern Thailand 14

2.4 Permeability of intact rock 18

2.5 Effect of confining pressure on permeability and porosity 22

2.6 Effect of compaction on sandstone porosity 30

2.7 Permeability and porosity relationship of rock 32

มหาวิทยาลัยเทคโนโลยีสุรนารี

TABLE OF CONTENTS (Continued)

Page

2.8 Stress dependent specific storage 34

2.9 Permeability anisotropy 35

2.10 Petrographic and classification of sandstones 37

III SAMPLE PREPARATION 39

3.1 Introduction 39

3.2 Sample preparation 39

3.3 Thin section 48

3.4 Petrographic analysis 49

IV TESTING METHODS AND RESULTS 52

4.1 Introduction 52

4.2 Test apparatus and method 52

4.3 Test results 54

4.4 Permeability Calculation 65

4.5 Effective Porosity Calculation 66

4.6 Discussions and Conclusions 70

V POTENTIAL APPLICATION 72

5.1 Introduction 72

5.2 Permeability-Porosity relationship under confining pressure .. 72

5.3 Volumetric changes 74

5.4 Formation compressibility 75

มหาวิทยาลัยเทคโนโลยีสุรนารี

TABLE OF CONTENTS (Continued)

Page

5.5 Storativity of sandstone 77

5.6 Discussions and Conclusions 78

VI DISCUSSIONS AND CONCLUSIONS 80

6.1 Discussions 80

6.2 Conclusions 82

6.3 Recommendations for future studies 83

REFERENCES 85

BIOGRAPHY 93

มหาวิทยาลัยเทคโนโลยีสุรนารี

LIST OF TABLES

Table		Page
2.1	Summary of pumping test data (DMR,1992).	15
2.2	Permeability of associated rock formations obtained elsewhere	24
2.3	Summary of experimental results on other sandstones	31
3.1	Specimens with bedding planes parallel to main axis	41
3.2	Specimens for Phu Phan sandstone with core axis normal to bedding plane	42
3.3	Specimens for Sao Khua sandstone with core axis normal to bedding plane	42
3.4	Saturated sandstone specimens	47
3.5	Summary of petrographic analysis	50
3.6	Summary of petrographic analysis (continued)	51
4.1	Summary of test results	65
4.2	Summary of empirical constants	68
4.3	Specimen diameters and lengths before and after testing for Phu Phan sandstone with parallel to bedding planes	69
4.4	Specimen diameters and lengths before and after testing for Phu Phan sandstone with normal to bedding planes	69
4.5	Specimen diameters and lengths before and after testing for Sao Khua sandstone with parallel to bedding planes	70
4.6	Specimen diameters and lengths before and after testing for Sao Khua sandstone with normal to bedding planes	70

LIST OF TABLES (Continued)

Table **Page**

5.1 Summary of empirical constants 74

5.2 Volumetric change of specimens under each confinement for Phu Phan and Sao Khua sandstone 75

5.3 Constants used to calculate sandstone formation compressibility 77

5.4 Summary of constant to calculated storativity of sandstone 78

มหาวิทยาลัยเทคโนโลยีสุรนารี

LIST OF FIGURES

Figure **Page**

1.1 Research methodology 4

2.1 Stratigraphy and revised age dating of the Khorat Group 9

2.2 Road-cut outcrop of the study area showing rock units no.1-4 (photo taken to the south) 10

2.3 Intact rock with voids, where possible flow occurs through interconnected voids. (b) Specimen with a major discontinuity, where flow occurs through discontinuity and any interconnected voids 19

2.4 TAW-1000 Electro-hydraulic Servo Controlled Testing System: (a) Loading System, (b) Main Switches, (c) Presure Pumps 21

2.5 Sample Assembly 21

2.6 Stress dependent (a) permeability and (b) porosity of the sandstone and silty-shale for sandstone (red dashed lines) and silty-shale (solid black lines) 25

2.7 Loading and unloading curves of the stress dependent permeability and porosity for sandstone (a), (c) and silty-shale (b), (d). Both an exponential relationship and a power law were utilized to fit the experimental data 27

2.8 Porosity and permeability as a function effective confining pressure curve with curve fit for a representative reservoir sandstone samples (a), (b) and (c) and (d) for reservoir limestone samples 31

2.9 Confining pressure relate to porosity 32

LIST OF FIGURES (Continued)

Figure **Page**

2.10 Stress dependent specific storage calculated based on an exponential relationship (a) and power law (b) 36

3.1 Laboratory core drilling. Core drilling machine (model SBEL 1150) used to prepare core specimens using diamond impregnated bit with diameter of 54 mm 40

3.2 Core specimen cut to length by a cutting machine 41

3.3 Phu Phan sandstone specimens with core axis parallel bedding plane 42

3.4 Sao Khua sandstone specimens with core axis parallel bedding plane 43

3.5 Phu Phan sandstone specimens with core axis normal to bedding plane 43

3.6 Sao Khua sandstone specimens with core axis normal to bedding plane 43

3.7 Rock specimens saturated in vacuum-chamber at a negative pressure of 0.1 MPa for 48 hours 44

3.8 Water contents of Phu Phan sandstone specimens as a function of time 45

3.9 Water contents of Sao Khua sandstone specimens as a function of time 46

3.10 Cut-off to the slide by using thin section saw 48

3.11 Thin section slides of Phu Phan and Sao Khua sandstones in directions normal (a),(c) and parallel (b),(d) to bedding planes 49

4.1 Laboratory arrangement scheme for constant head flow test under high confining pressures 53

4.2 Laboratory setup for constant head flow test under high confining pressures 53

LIST OF FIGURES (Continued)

Figure **Page**

4.3 Flow rates normal to bedding planes as a function of time for confining pressures at 10 MPa for Phu Phan sandstone 54

4.4 Flow rates normal to bedding planes as a function of time for confining pressures at 20 MPa for Phu Phan sandstone 55

4.5 Flow rates normal to bedding planes as a function of time for confining pressures at 30 MPa for Phu Phan sandstone 55

4.6 Flow rates normal to bedding planes as a function of time for confining pressures at 40 MPa for Phu Phan sandstone 56

4.7 Flow rates normal to bedding planes as a function of time for confini pressures at 50 MPa for Phu Phan sandstone 56

4.8 Flow rates normal to bedding planes as a function of time for confining pressures at 10 MPa for Sao Khua sandstone 57

4.9 Flow rates normal to bedding planes as a function of time for confining pressures at 20 MPa for Sao Khua sandstone 57

4.10 Flow rates normal to bedding planes as a function of time for confining pressures at 30 MPa for Sao Khua sandstone 58

4.11 Flow rates normal to bedding planes as a function of time for confining pressures at 40 MPa for Sao Khua sandstone 58

4.12 Flow rates normal to bedding planes as a function of time for confining pressures at 50 MPa for Sao Khua sandstone 59

มหาวิทยาลัยเทคโนโลยีสุรนารี

LIST OF FIGURES (Continued)

Figure **Page**

4.13 Flow rates parallel to bedding planes as a function of time for confining pressures at 10 MPa for Phu Phan sandstone 59

4.14 Flow rates parallel to bedding planes as a function of time for confining pressures at 20 MPa for Phu Phan sandstone 60

4.15 Flow rates parallel to bedding planes as a function of time for confining pressures at 30 MPa for Phu Phan sandstone 60

4.16 Flow rates parallel to bedding planes as a function of time for confining pressures at 40 MPa for Phu Phan sandstone 61

4.17 Flow rates parallel to bedding planes as a function of time for confining pressures at 50 MPa for Phu Phan sandstone 61

4.18 Flow rates parallel to bedding planes as a function of time for confining pressures at 10 MPa for Sao Khua sandstone 62

4.19 Flow rates parallel to bedding planes as a function of time for confining pressures at 20 MPa for Sao Khua sandstone 62

4.20 Flow rates parallel to bedding planes as a function of time for confining pressures at 30 MPa for Sao Khua sandstone 63

4.21 Flow rates parallel to bedding planes as a function of time for confining pressures at 40 MPa for Sao Khua sandstone 63

4.22 Flow rates parallel to bedding planes as a function of time for confining pressures at 50 MPa for Sao Khua sandstone 64

มหาวิทยาลัยเทคโนโลยีสุรนารี

LIST OF FIGURES (Continued)

Figure **Page**

4.23 Intrinsic permeability as function of confining pressures 67

4.24 Effective porosity in directions normal and parallel to bedding plane as a function of confining pressures 68

5.1 Permeability – Porosity relation empirical equation 73

5.2 Volumetric change as a function of confining pressure 76

มหาวิทยาลัยเทคโนโลยีสุรนารี

SYMBOLS AND ABBREVIATIONS

β	=	The compressibility of water (4.4×10^{-10} Pa^{-1})
γ_w	=	The unit weight of water (9,789 N/m^3)
Δ	=	The volumetric change (%)
η	=	Empirical constants
μ	=	The dynamic viscosity of water (1.005×10^{-3} $N\cdot s/m^2$)
ρ_w	=	Density of water (g/cm^3)
σ_3	=	The confining pressure (MPa)
°C	=	The degree Celsius
$\Delta h/L$	=	The hydraulic head gradient
*P	=	The pore space
a	=	Constants
A	=	The cross-section area of flow (m^2)
b	=	Constants
c_f	=	The formation compressibility (GPa^{-1})
d	=	The dry weight of specimen (g)
Fsp	=	Feldspar
g	=	The gravitational acceleration (9.8 m/sec^2)
K	=	The bulk modulus (GPa)
k	=	The intrinsic permeability (m^2)
k_h	=	The horizontal permeability (m)
k_v	=	The normal permeability (m^2)

มหาวิทยาลัยเทคโนโลยีสุรนารี

SYMBOLS AND ABBREVIATIONS (Continued)

k_0	=	The rock permeability under zero confinement (m^2)
K_{hc}	=	The hydraulic conductivity (m/s)
k_h/k_v	=	The permeability anisotropy
n_e	=	The effective porosity (%)
Q	=	The flow rates (m^3/s)
Qtz	=	Quartz
S	=	The storativity
S_s	=	The specific storage (m^{-1})
t	=	The aquifer thickness (m)
V	=	The total bulk volume of specimen (cm^3)
V_0	=	The original volume (m^3)
V_a	=	The new volume (m^3)
W	=	The saturated weight of specimen (g)
w_{ave}	=	The average water contents (%)

มหาวิทยาลัยเทคโนโลยีสุรนารี

CHAPTER I

INTRODUCTION

1.1 Background and rationale

For intact rock without any fractures, the fluid will flow through the small pores, which are randomly distributed in its matrix. The hydraulic and mechanical behaviors for the intact rock can be described by continuum mechanics like soil, which are relatively straightforward (Wong et al, 1997). Permeability is a measure of the ability of a porous media to transmit fluids. It is important controlling parameter of fluid flow systems in the rocks (Whitaker, 1986). This parameter is particularly important in sandstones since they generally are either groundwater or petroleum reservoirs. At greater depths, the permeability of the rocks tends to reduce due to higher stresses (Sukplum et al, 2013). The mechanical behavior and structural expression of deformation in a porous sandstone may be influenced by many competing factors, including porosity, mineralogy, pore fluid and confining pressure (Wong et al., 1997; Baud et al., 2000). It has been commonly found that the confining pressure can notably reduce the effective porosity of rocks, and subsequently decrease their permeability (Ghabezloo et al., 2009; Dong et al., 2010; Huiyuan et al., 2016). This finding has been concluded from many flow tests conducted in the laboratory under controlled hydrostatic pressures.

Most of the previous researchers have been concentrated on the effects of confining pressure and pore pressure on the permeability of rock. Wannakao, et al. (2010) estimate the coefficient of permeability of Phra Wihan, Phu Phan and Nam Phong formations

under confining pressures by using flowing water with different pressures at inlet and outlet positions. The results indicate that the permeability reduces as the confining pressures increase. The equation used to estimate permeability based on porosity is proposed as $k = 9.68n^{1.899}$, where k is permeability (mD or millidarcy; 1 mD = 9.87×10^{-16} m^2) and n is fraction porosity. The significant variables affected the permeability of rock are porosity, mineral composition and thickness of cross bedding (Wannakao et al., 2014). The permeability increases with effective grain size and porosity increase. Sukplum (2012) studies anisotropy permeability by flowing gas and water under confining stresses from 4 to 16 MPa. The specimens are collected from the Nam Phong formation.

The heterogeneity of rock permeability is measured in two directions, parallel and perpendicular to lamination or cross bedding of specimens. The results indicate that the permeabilities of rock samples are very low. The water permeability ranges from less than 9.87×10^{-19} m^2 to 3.35×10^{-16} m^2, while the gas permeability range from less than 1 μDarcy to 59.25 μDarcy. The anisotropic water permeability (k_h/k_v) range from 0.30-18.54 and anisotropy infinite permeability ($k_{\infty h}/k_v$) range from 0.19-2.26. Several models used to describe the relations between confining pressure and permeability have been proposed by several researchers, including exponential, power law and polynomial relations (David et al., 1994; Zisser and Nover, 2009; Dong et al., 2010; Zhijiao et al., 2014). Even though there have been several experiments performed to determine the permeability of these Thai sandstone formations. They are mostly conducted under relatively lower confining pressures, and hence the results may not represent the rock permeability under great depths.

1.2 Research objectives

The objective of this study is to investigate the effective permeability and porosity of Sao Khua and Phu Phan sandstone formations. The main efforts involve conducting laboratory flow tests to determine the hydraulic performance of the sandstones and the confining pressures are determined under 10 to 50 MPa (2 kilometers depth). The sample preparation follows the ASTM standards (ASTM D4543-08) with a nominal dimension of 5.4 cm in diameter and 8.1 cm in length. They are prepared with the axis normal and parallel to the bedding plane. A minimum of 12 specimens are prepared for each rock type. The permeability coefficient (K) can be calculated by ASTM (D2434-68). The results are used to assess the yield pumping rate, and anisotropic of permeability is applied to describe flow path by petrological analysis.

1.3 Research methodology

The research methodology shown in Figure 1.1 comprises 8 steps; including literature review, sample collection and preparation, constant head flow test, petrographic analysis of thin sections, analysis and assessment, application, discussions and conclusions and thesis writing.

มหาวิทยาลัยเทคโนโลยีสุรนารี

1.3.1 Literature review

Literature review is carried out to study researches on the stratigraphy of sandstone formations in the northeast Thailand, stress-dependent permeability and porosity, anisotropy permeability, petrological of sandstone and pumping well. The sources of information are from textbooks, journals, and conference papers. A summary of the literature review is given in the thesis.

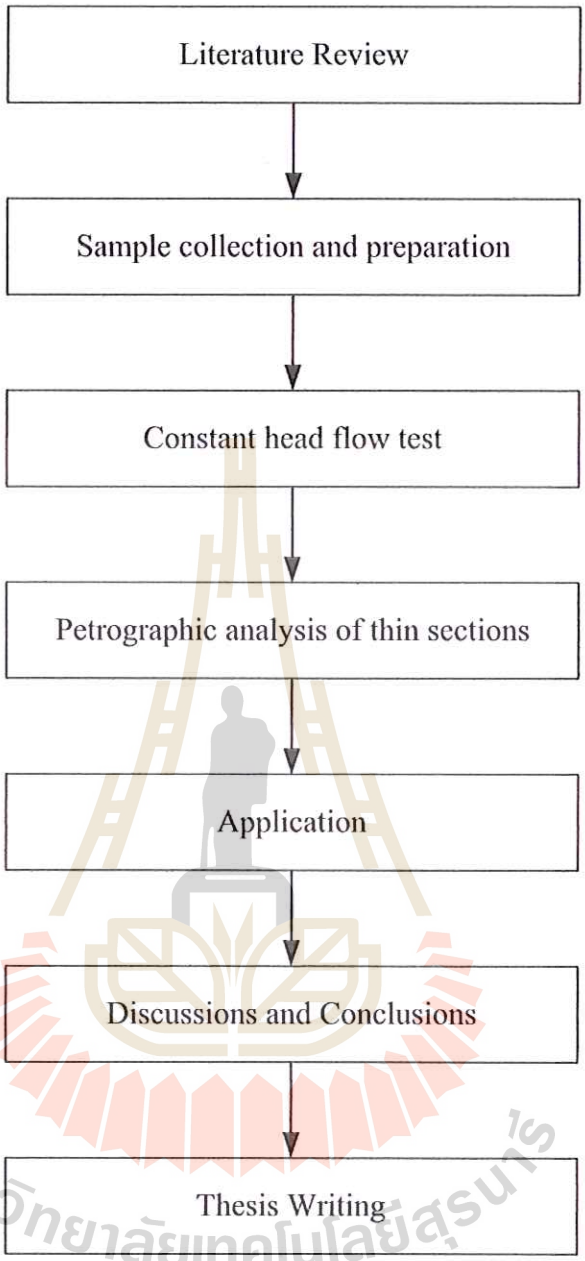

Figure 1.1 Research Methodology

มหาวิทยาลัยเทคโนโลยีสุรนารี

1.3.2 Sample preparation

The rock specimens belong to Phu Phan and Sao Khua formations. The Phu Phan sandstones are fine-grained comprising 80% quartz, 2.5% feldspar, 5.5% rock fragment, 1.5% mica and 10.5% other. Sao Khua sandstones are very fine-grained comprising 58% quartz, 5.5% feldspar, 7.5% rock fragment, 3% mica and 26% other (Racey,1996). The specimen density is averaged as 2.4±0.1 g/cc. The sample preparation follows the ASTM standards (ASTM D4543-08) with nominal dimensions of 54 mm in diameter and 81 mm in length. A total of 12 specimens are prepared for each rock types.

1.3.3 Constant head flow test

The specimens are dried at 100 °C in an oven, and saturation in a vacuum-chamber at a negative pressure of 0.1 MPa for 48 hours before testing. A constant diameter water pump is used to inject water pressure to one end of the specimen. The specimen is placed in triaxial cell which is used to applied constant confining pressures to the rock specimen. The confining pressures are varied from 10 to 50 MPa.

1.3.4 Petrographic analysis of thin sections

Petrographic examinations are made for following purposes:

(1) minerals identification

(2) shape and grain size of minerals

(3) pore distribution

(4) sorting

มหาวิทยาลัยเทคโนโลยีสุรนารี

4 thin-sections are made from 4 core rock specimens, 2 thick-sections are parallel to bedding or cross-laminar and 2 thin-sections are perpendicular. The thin sections preparations are carried out and examined at Suranaree University of Technology.

1.3.5 Applications

The laboratory testing can be applied for sandstone aquifers to determine the storativity for sandstone aquifer considering the compressibility and elasticity of the rocks. The empirical equation of porosity and permeability relationship is used to determine formation compressibility and specific storage

1.3.6 Discussions and Conclusions

Discussions are made on the reliability and adequacies of the test data and the correctness of the interpretation and analysis. Future research needs are identified.

1.3.7 Thesis writing

All research activities, methods, and results are documented and complied in the thesis.

1.4 Scope and limitations

The scope and limitations of the research include as follows.

1. This research emphasizes the determination of hydraulic properties of sandstones.
2. The effective porosity and permeability of Phu Phan and Sao Khua sandstones under the confining pressures are determined under 10 to 50 MPa (depths = 400-2,000 m).
3. The laboratory test is measured permeability of sandstones by constant head flow test.

4. The test is performed on rock core nominal diameters of 54 mm and length to diameter ratio of 1.5.
5. A total of 24 specimens are tested.
6. No field testing is conducted.
7. The testing procedure will follow the relevant ASTM standard practice, as much as, practical.
8. The research findings are published in conference paper or journal.

1.5 Thesis contents

This first chapter introduces the thesis by briefly describing the rationale and background and identifying the research objectives. The third section identifies the research methodology. The fourth section describes scope and limitations. The fifth section gives a chapter by chapter overview of the contents of this thesis. The second chapter summarizes results of the literature review. Chapter three describes samples preparation. The methods and results of the laboratory testing are described in chapter four. Chapter V describes the application of this research. Chapter VI summarizes the research results, and provides recommendations for future research studies.

มหาวิทยาลัยเทคโนโลยีสุรนารี

CHAPTER II

LITERATURE REVIEW

2.1 Introduction

This chapter gives the results of literature review carried out to improve an understanding of the stratigraphy of northeast Thailand, permeability and porosity of sandstones studied here. The topics include stratigraphy of northeast Thailand, potential of groundwater in Korat Plateau, permeability of intact rock, effect of confining pressure on permeability and porosity, permeability anisotropy and petrographic and classification of sandstones.

2.2 Stratigraphy of northeast Thailand

The Khorat group is traditionally considered to comprise from bottom to top, Nam Phong, Phu Kradung, Phra Wihan, Sao Khua, Phu Phan and Khok Kruat formations (Racey and Goodall, 2009). The group is unconformably overlain by the continental evaporitic Maha Sarakham formation, which has been palynologically dated as mid-Albian–Cenomanian, therefore giving a minimum age for the underlying Khorat group. Traditionally the Nam Phong formation is considered to be Late Triassic, Phu Kradung, Phra Wihan and Sao Khua formations are assigned to the Jurassic, and Phu Phan and Khok Kruat formations to the Early Cretaceous, as shown in Figure 2.1.

Songsawad and Chutakositkanon (2009) investigates the sedimentary rocks in Khao Phang Hoei Changwat Chaiyaphum. This area can be divided into four units, as shown in Figure 2.2. The strata in the investigated area can be simply grouped into one

Previous Workers (Department of Mineral Resources Thailand (1992) and Sattayarak & Srigulawong (2008)				This Work			
Age		Lithostratigraphy		Age			Lithostratigraphy	
Cretaceous	Late	Khorat Group	Maha Sarakham Formation	Cretaceous	Late	Albian to Cenomanian	Maha Sarakham Formation	
	Early		Khot Kruat Formation		Early	Aptian	Khorat Group	Khot Kruat
						Undifferentiated Early Cretaceous		Phu Phan
			Phu Phan Formation			Berriasian to Early Barremian		Sao Khua
								Phra Wihan
								Phu Kradung
Jurassic	Late		Sao Khua Formation		Late	(Phu Kradung may in part be latest Jurassic)	Upper Nam Phong Formation	
	Middle		Phra Wihan Formation	Jurassic			?—?—?—?	
	Early		Phu Kradung Formation					
Triassic	Late		Nam Phong Formation	Triassic	Late	Late Norian to Rhaetian		Lower Nam Phong Formation

Figure 2.1 Stratigraphy and revised age dating of the Khorat Group (DMR, 1992; Sattayarak and Srigulawong, 2008; Racey and Goodall, 2009).

มหาวิทยาลัยเทคโนโลยีสุรนารี

Figure 2.2 Road-cut outcrop of the study area showing rock units no.1-4 (photo taken to the south) (Songsawad and Chutakositkanon, 2009).

major sequence based upon physical properties and lithological association, as red clastic rocks. This unit can be correlated with some part of Sao Khua formation in the Khorat group. The rocks are characterized by reddish brown to purple siltstones, mudstones with calcrete nodules and bioturbation burrows, conglomeratic to very fine-grained reddish brown to greyish white well-sorted with many sedimentary structures such as graded bedding, cross bedding, and cross-lamination. The depositional environment of sedimentary rocks in Khao Phang Hoei area indicate pertains to meandering rivers and floodplain in semiarid to arid paleoclimate.

In the following section, the studied formations are described in terms of their general lithology, detailed petrography, stratigraphic relationships and thickness, environment of deposition (Racey et al., 1996).

2.2.1 Sao Khua Formation descriptions

2.2.1.1 Lithology

This formation consists of common fluvial sandstones and flood-plain mudstones, together with rarer, sand-matrix supported caliche conglomerates. The sandstones are usually fine grained and tightly cemented, although carbonate cemented conglomerate beds are present locally. Red-brown and purple-grey

friable siltstones and mudstones are common, and often contain calcareous nodules, gastropods, bivalves and occasional dinosaur remains.

2.2.1.2 Petrography

The sandstones are classified mainly as lithic arenites and are often calcareous. Grain sizes range from fine-sand to pebble grade (mean values of fine sand). The sorting is highly variable, ranging from poor to good. Grain shapes range from sub-angular to sub-rounded. Compaction effects range from low to moderate, with grains showing point or long contacts. Rare, deformed mica flakes are also present. In thin section, the sandstones generally appear unstructured.

2.2.1.3 Detrital Mineralogy

- **Quartz:** mainly comprises monocrystalline grains, which often show streaks rich in fluid inclusions. Polycrystalline grains are sparse and consist of sutured crystal mosaics that are rarely porphyroblastic.
- **Feldspar:** is generally rare and consists of partially etched and kaolinitised orthoclase and plagioclase grains.
- **Rock fragments:** include grains of igneous quartz and feldspar crystal aggregates.
- **Other:** Micas are exclusively composed of relatively unaltered laths of muscovite. Heavy minerals include angular to euhedral zircon, sub-angular tourmaline and rutile, and rounded apatite. Optically non-resolvable clay minerals are dominated by sparse, brown, amorphous pore-filling aggregates, which probably represent a detrital matrix.

มหาวิทยาลัยเทคโนโลยีสุรนารี

2.2.1.4 Stratigraphic Relationships and Thickness

The Sao Khua Formation conformably overlies the Phra Wihan Formation and is conformably overlain by the Phu Phan Formation. The formation is 720 m thick at the type locality at km 35 on the Udon Thani Nong Bua Lamphu Road (Ward and Bunnag, 1964). The Sao Khua Formation ranges in thickness from 200-760 m in general with the average thickness at the Phu Phan range of about 120 m (50-200 m). The Sao Khua Formation composed of various cycles of reddish brown silty claystones interbedded with siltstones, fine- to medium-grained sandstones and conglomerates, and caliches, calcrete nodules, thin-bedded and nodular silcretes (Meesook et al., 2002).

- **Depositional Environment**

The Sao Khua formation is considered as the deposits in the big, shallow clay pans or lacustrine basins with psammitic flood-plain sediments, occasionally, river channel deposits cut into the underlying argillaceous sediments (Sattayarak, 1983). They are interpreted to have been deposited in low- energy, meandering fluvial channels and extensive floodplains which are modified by pedogenesis. Thinner sandstone beds are interpreted to represent crevasse splays, and those more than 1.5 m thick represent meandering channels.

2.2.2 Phu Phan Formation descriptions

2.2.2.1 Lithology

The formation consists of medium to coarse grained (locally conglomeratic) fluvial sandstones and floodplain siltstones and mudstones. The sandstones are light-buff to brown, and trough and planar cross-bedded. The sandstones are often stacked into 15-40 m thick units. Owing to its generally coarser grain size,

the reservoir quality of the Phu Phan Formation is better than that of the underlying formations of the Khorat Group. The contact with the underlying Sao Khua Formation is generally erosive and is often marked by matrix-supported conglomerates rich in is generally erosive and is often marked by matrix-supported conglomerates rich in caliche clasts. Red silty clay stones and caliche are occasionally observed and are interpreted as floodplain deposits.

2.2.2.2 Petrography

Sandstones from the Phu Phan Formation consist mainly of quartz arenites and less common arkosic arenites. Some of the sandstones contain >10.0% authigenic silica. Grain sizes range from very fine to coarse sand grade, while the sorting is moderate to good. Grain shapes range between sub-angular and sub-rounded. Compaction ranges from low to high (mainly moderate). Grain contacts vary from point to locally sutured, but straight or concavo-convex contacts are more common. Most of the samples appear unstructured in thin section.

2.2.2.3 Detrital Mineralogy

- **Quartz:** is dominated by monocrystalline, often inclusion-rich grains, which show straight to strongly zoned extinction. Polycrystalline grains are composed of sutured, often foliated crystals, which locally appear inclusion-rich.

- **Feldspar:** is dominated by alkali feldspar, comprising etched and honeycombed orthoclase grains. Plagioclase grains are rare and are often almost totally leached or replaced by kaolinite.

- **Rock fragments:** include rare volcanic grains, with metapelite and quartz-mica schist fragments recorded locally.

- **Other:** Micas are represented exclusively by relatively fresh and unaltered laths of muscovite. Heavy minerals are rare, and include rounded grains of rutile, tourmaline, zircon and epidote. Optically non-resolvable clay minerals are rare, and mainly consist of brown, amorphous, pore-filling detrital matrix.

2.2.2.4 Stratigraphic Relationships and Thickness

This formation conformably overlies the Sao Khua Formation and is conformably overlain by the Khok Kruat Formation. The formation is 183 m thick at the type locality at Phu Pha Phung in the Phu Phan Range of NE Thailand (Ward and Bunnag, 1964).

- **Depositional Environment**

Sandstones within the formation are interpreted to have been deposited in braided, high energy, low sinuosity river channels. The subordinate finer-grained sediments represent floodplain and abandonment fines. The bedload transported by these rivers is, overall, the coarsest of any of the Khorat Group sandstones examined in this study. Localized slumping and folding below coarse-grained, cross-bedded sets indicates very rapid deposition in high-energy conditions.

2.3 Potential of groundwater in the northeastern Thailand

Groundwater in the northeastern Thailand occurs mainly in cracks, joints, faults (fractures), and bedding planes of shale, siltstone and sandstone of the Khorat Group which is mainly underlain the Khorat Plateau. No primary porosity of these rocks is of any value for groundwater storage sine the primary permeability of the coarse grain sandstone is tested at 0.00008 m^2/day or less. Groundwater resources in each aquifer has a wide range in both quantity and quality. It depends upon the aquifers rock types,

Table 2.1 Summary of pumping test data (DMR,1992).

Aquifers	Pumping test		Yield range (m^3/hr)	Transmissivity (m^2/day)	
	Average tube well depth (m)	No. of wells		Range	Average
Phu Tok	30-150	38	5-204	0.5-2955	500
Mahasarakham	40-60	10	5-20	20-290	100
Khok Kruat	30-80	17	3-15	0.4-11.6	4.7
Phu Phan	25-60	8	4-10	0.5-15	9.6
Sao Khua	50-180	15	5-10	2.5-50	29
Phra Wihan	40-60	3	2-8	0.3-10	8.5
Phu Kradung	30-60	24	10-40	3.5-1000	300
Nam Phong	40-60	2	3-8	0.5-10	5

and geological structures. Table 2.1 shows pumping test, yield range and transmissivity in each aquifer (DMR,1992).

Piancharoen (1973) classified the aquifers of the northeastern Thailand on the 1:500,000 Hydrogeological Map according to their rock types and water - bearing characteristics from younger to older namely, Unconsolidated, Upper Khorat, Rat Buri limestone and Metasediment aquifers. The Upper Khorat aquifer (Cretaceous) is consisted of red, reddish brown and grayish brown shale, siltstone and sandstone of salt and Khok Kruat Formations. Groundwater of this aquifer variable in both quantity and quality. In the flood plain and relatively flat land, efflorescence salt commonly occurs on the ground surface, and more than 90% of drilled wells yield salty water. Middle Khorat aquifer (Jurassic) is consisted of yellowish gray to grayish pink massive sandstone and conglomerate of Phu Phan formation on top; grayish red to olive gray to white massive thick bedded quartzose sandstone of Phra Wihan Formation at bottom; with dark reddish brown to brownish gray shale and siltstone of Sao Khua Formation in between. In the escarpment regions, groundwater can be developed from the middle

Khorat aquifer along dip slopes or strike valleys. Yields of about 1-5 m^3/hr of exceptionally good quality water may be obtained from the wells drilled at 200 m. Many wells are of artesian flowing with rate up to 5 m^3/hr. The most recent studied of the hydrogeology and groundwater resources of the Northeast has classified the aquifers ofthe northeastern Thailand as following:

Phu Phan Aquifer: The unit is characterized by thick, resistant, massive coarse quartz sandstone, with some conglomeratic horizons. The unit which varies from 100-400 m in thickness was deposited during Lower Cretaceous and forms nearly flat top hills to undulating terrain. Recharge to the aquifer occurs by direct infiltration of rainfall where the more permeable unit outcrop of subcrop. Groundwater flowing is down dip, becoming through the overlying formations and along foully zones. Yield ranges of 1-10 m^3/hr can be expected from drilled well penetrated to fractured zone of aquifer. The transmissivity values ranging between 10-40 m^2/day. Groundwater is generally good quality occasionally high iron contents. Most wells drilled in Phu Phan aquifer are non-flowing artesian although several flowing wells have been drilled.

Sao Khua Aquifer: The Sao Khua aquifer is composed of purplish to friable micaceous sandstone and siltstone, varying in thickness from 400-720 m. It has very low resistance to weathering and forms areas of flat to undulating topography. Yield from borehole in Sao Khua aquifer range from 5-10 m^3/hr with exceptionally good quality water may be obtained from the well drilled at 200m. Many wells are of artesian flowing with rate up to 30 m3/hr. Transmissivity values ranging between 2.5-50 m^2/day were obtained from 15 pumping tests. The various aquifers occurring in the Northeast can be divided into three broad classes (DMR,1992).

Class I: Aquifers providing large yields of high quality water suitable for most

uses. These belongs to the Tertiart-Cretaceous Phu Tok aquifer, Phu Kradung aquifer, Carbonate aquifer or Ratburi limestone aquifer and Terrace deposits aquifer.

Class II: Aquifer providing low to medium yield of good to moderate quality groundwater suitable possibly for village water supply and for small scale irrigation. The aquifer in this case belong to Sao Khua, Phu Phan, Khok Kruat, Phra Wihan aquifers.

Class III: Aquifers containing essentially brackish to saline or limited groundwater with varying yields. Aquifers within the flood alluvium Mahasarakham aquifers and igneous rocks aquifers to this group. For Phu Phan and Sao Khua aquifers: these aquifers are relatively good quality water and individual drilled well yield up to 20 m3/hr suggest that the groundwater resources of the aquifers within these aquifers has potential for development for village water supply and for local small-scale irrigation as well as industry. The Phu Phan aquifer is a source of spring discharge and a large spring has been developed as a gravity water supply for many areas as Amphoe Mancha Khiri. Both fractured siltstone and sandstone occur within the Sao Khua aquifer and yield of good quality water of up to 30 m3/hr have been obtained from drilled wells 180 m deep. Ground water under artesian pressure probably occurs in several of the more permeable sandstone beds dipping from the margin to the central part of the Khorat Plateau. The most important are the medium- and coarse-grained sandstone beds in the Phu Phan and Phra Wihan members of the Khorat series (LaMoreaux, et al, 1958).

2.4 Permeability of intact rock

Darcy carries out experiments on flow through packs of sand and hence developed an empirical formula that remains the main permeability formula in use in the oil industrial today. It has since been validated for most rock types and certain common fluid. Darcy's formula can be expressed as:

$$K = Q / A(\Delta h/L) \tag{2.1}$$

where K is hydraulic conductivity (m/s), Q is flow rate (m^3/s), A is a cross-section area of flow (m^2), γ_w is unit weight of water (9,789 N/m^3), and $\Delta h/L$ is hydraulic head gradient.

For crystalline rocks, fluid flow through rock matrix is much less than that through fractures, because the extent of interconnected pores and the pore sizes in hard rocks are generally small. Permeability can greatly influence the mechanical behavior of rocks, thereby increasing or decreasing the stability of rock structures. As shown in Figure 2.3, fluid flow within a rock specimen can take place through either the rock matrix or interconnected discontinuities or combination of both. Under single-phase fluid flow, permeability can be divided into three main categories: (1) Matrix permeability, (2) Fracture permeability and (3) Dual permeability and the calculation of permeability is as follows (Indraratna and Ranjith, 2001).

$$K = \rho g k/\mu \tag{2.2}$$

where K is hydraulic conductivity, ρ is density of the fluid, g is acceleration of gravity, k is the coefficient of permeability and μ is the dynamic viscosity of the fluid.

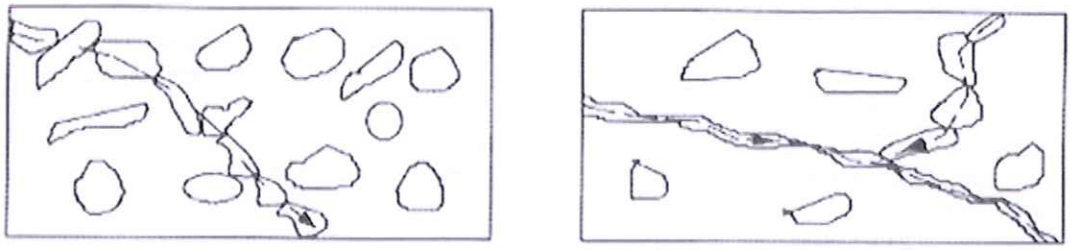

(a) (b)

Figure 2.3 (a) Intact rock with voids, where possible flow occurs through interconnected voids. (b) Specimen with a major discontinuity, where flow occurs through discontinuity and any interconnected voids (Indraratna and Ranjith, 2001).

Yu et al. (2016) study mechanical properties and permeability of a single jointed sandstone with filling are experimentally investigate using a TAW-1000 electro-hydraulic servo-controlled testing system (Figure 2.4). The testing system could independently and precisely control the axial loading, confining pressure and pore pressure, with the aid of three independent closed loops. The maximum vertical loading capacity of the system is 1000 kN (with an error of ±5 N), which is equivalent to about 509 MPa considering the specimen area, and the maximum confining and pore pressures are 70 and 40 MPa, respectively, with an accuracy of ±0.01 MPa. The testing system is also capable of performing permeability tests of rock and concrete.

Before the triaxial testing and permeability testing are conducted, the saturated rock samples are sealed with adhesive tape and jacketed in impervious Teflon heat-shrink tubing. The jacket prevents the pressure fluid from entering the pores or cracks, and to effectively enable the confining pressure to inhibit the opening of cracks or sliding on existing crack surfaces. At this point, resistor strain type displacement

transducers for axial and radial strain measurements, whose measurement ranges respectively are 4 and 2 mm, and whose accuracies are less than ±0.001 mm, are installed, and the assembled sample was placed into the chamber on the lower platen of the load frame (Figure 2.5). Then, the pipeline and data lines were connected. Finally, the assembled sample was covered and sealed by a confining pressure cell, into which silicone oil was injected. When all steps are completed, the load was applied by computer. All triaxial tests are performed with the confining pressure of 20 MPa during the loading process. It should be noted that the effects of temperature were not studied here. All the tests were carried out under isothermal conditions at room temperature (20±30 °C).

Permeability depends mainly on the porosity, connectivity and tortuosity of the porous network. In the case of the sandstone studied here, its initial permeability is relatively high (10^{-16} m^2), thus the steady-state flow method rather than the pulse-test method is used (Brace et al., 1968). In these experiments, we assume that the classic Darcy's law is valid, and from the flow rate Q (m^3/s) we calculate the permeability according to the following formula:

$$k = Q\mu L/\Delta pA \tag{2.3}$$

where μ (Pa·s) is the dynamic viscosity coefficient of distilled water, and is equal to 1.005×10^{-3} Pa·s under a room temperature of 20°C; L (m) and A (m^2) stand for the height and cross-section of the rock samples, respectively; and Δp (Pa) is the pressure gradient between the end-faces of the rock cores, and is set at 5 MPa in this research.

(a) (b) (c)

Figure 2.4 TAW-1000 Electro-hydraulic Servo Controlled Testing System: (a) Loading System, (b) Main Switches, (c) Pressure Pumps (Yu et al., 2016)

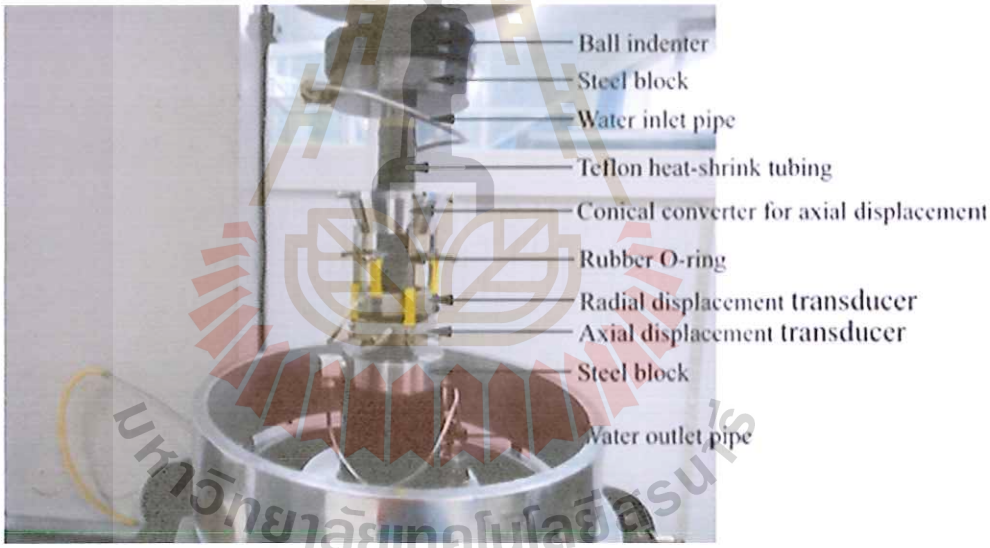

Figure 2.5 Sample Assembly (Yu et al., 2016).

2.5 Effect of confining pressure on permeability and porosity

The literatures are reported that the permeability of porous media generally decreases with increasing effective stresses, but the permeability measurements can be performed under different stress conditions: hydrostatic and non-hydrostatic stress conditions. In a hydrostatic test, the axial stress is equal to the confining stress. Non-hydrostatic test can for example be triaxial compression test or constant stress ratio test (Shijia,2017).

For intact rock without any fractures, the fluid will flow through the small pores,which are randomly distributed in its matrix. The hydraulic and mechanical behaviors for the intact rock can be described by continuum mechanics like soil, which are relatively straightforward.

Permeability is measurement of the ability of a porous media to transmit fluids. It is an important controlling parameter of fluid flow systems in the rocks. This parameter is particularly important in sandstones since they generally are either groundwater or petroleum reservoirs. At greater depths, the permeability of the rocks tends to reduce due to higher stresses (Sukplum et al., 2013). The mechanical behavior and structural expression of deformation in a porous sandstone may be influenced by many competing factors, including porosity, mineralogy, pore fluid and confining pressure (Wong et al., 1997; Baud et al., 2000). It has been commonly found that the confining pressure can notably reduce the effective porosity of rocks, and subsequently decreases their permeability (Ghabezloo et al., 2009; Dong et al., 2010; Huiyuan et al., 2016). This finding has been concluded from many flow tests conducted in the laboratory under controlled hydrostatic pressures. Most of the previous researchers have been concentrated on the effects of confining pressure and pore pressure on the

permeability of rock. Wannakao et al. (2010) estimate the coefficient of permeability of Phra Wihan, Phu Phan and Nam Phong formations under confining pressures by using flowing water with different pressures at inlet and outlet positions. The results indicate that the permeability reduces as the confining pressure increases. The equation used to estimate permeability based on porosity is proposed as $k = 9.68n^{1.899}$, where k is permeability (mD or millidarcy; 1 mD = 9.87×10^{-16} m^2) and n is fractional porosity. The significant variables affecting the permeability of rock are porosity, mineral compositions and thickness of cross bedding (Wannakao et al., 2014). The permeability increases with effective grain size and porosity increase.

Sukplum et al. (2012) study the permeability by flowing gas and water under confining pressures from 4 to 16 MPa, using specimens from the Nam Phong formation. The anisotropy of rock permeability is measured in two directions (parallel and normal with bedding planes). The results indicate that the permeabilities of rocks sample are very low. The water permeability ranges from less than 1 to 340 μDarcy, while the gas permeability ranges from less than 9.87×10^{-19} m^2 to 5.84×10^{-11} m^2. The anisotropic water permeability $(k_{1//}/k_{1\perp})$ range from 0.30 to 18.54, and anisotropy infinite permeability $(k_{\infty//}/k_{\perp})$ ranges from 0.19 to 2.26 (Table 2.2). Several models used to describe the relation between confining pressure and permeability have been proposed by several previous researchers, including exponential, power and polynomial relations (David et al., 1994; Zisser and Nover, 2009).

Dong et al. (2010) integrate permeability and porosity measurement system to measure the stress dependent permeability and porosity of Pliocene to Pleistocene sedimentary rocks from a 2000 m borehole. Experiments are conducted by first gradually increasing the confining pressure from 3 to 120 MPa and then subsequently

Table 2.2 Permeability of associated rock formations obtained elsewhere (Sukplum, 2012)

Rock Formations	Confining Pressures (MPa)	Flow Directions	Permeability (m^2)	Porosity (%)	Permeability Anisotropy (k_p/k_n)
Namphong Formation (Khon Kaen Province)	4	Parallel	3.41×10^{-16}	4.38	19.73
		Normal	1.73×10^{-17}	4.48	
	8	Parallel	2.74×10^{-16}	3.94	18.82
		Normal	1.45×10^{-17}	4.06	
	12	Parallel	2.37×10^{-16}	3.55	17.74
		Normal	1.33×10^{-17}	3.55	
	16	Parallel	2.02×10^{-16}	3.69	16.07
		Normal	1.26×10^{-17}	3.34	
Namphong Formation (Loei Province)	4	Parallel	3.55×10^{-18}	2.66	1.29
		Normal	2.75×10^{-18}	2.71	
	8	Parallel	2.30×10^{-18}	2.15	1.15
		Normal	2.00×10^{-18}	2.24	
	12	Parallel	1.81×10^{-18}	1.74	1.23
		Normal	1.47×10^{-18}	1.86	
	16	Parallel	1.13×10^{-18}	1.33	1.25
		Normal	8.98×10^{-19}	1.47	
Namphong Formation (Chaiyaphum Province)	4	Parallel	1.02×10^{-17}	2.82	4.39
		Normal	2.33×10^{-18}	3.59	
	8	Parallel	6.72×10^{-18}	2.41	4.93
		Normal	1.36×10^{-18}	3.15	
	12	Parallel	5.13×10^{-18}	2.07	5.15
		Normal	9.97×10^{-19}	2.81	
	16	Parallel	4.02×10^{-18}	1.71	4.33
		Normal	9.28×10^{-19}	2.46	

มหาวิทยาลัยเทคโนโลยีสุรนารี

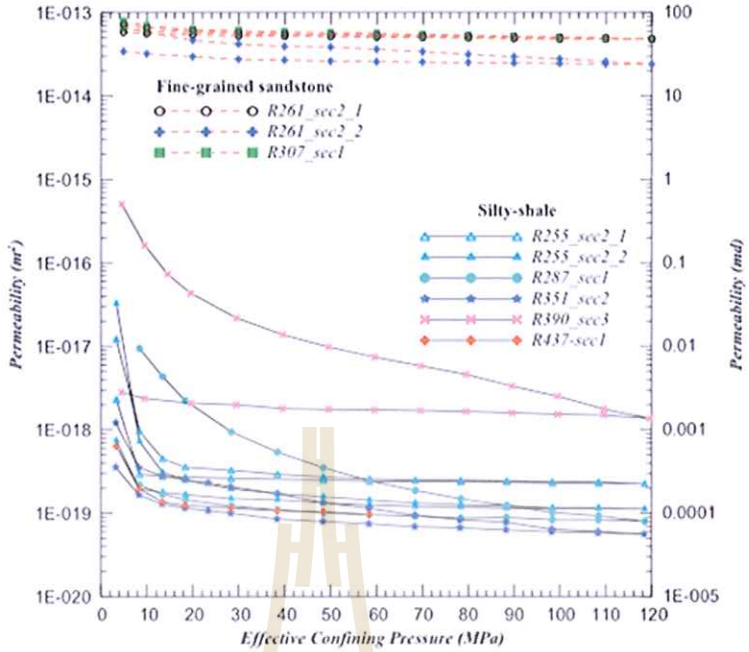

(a)

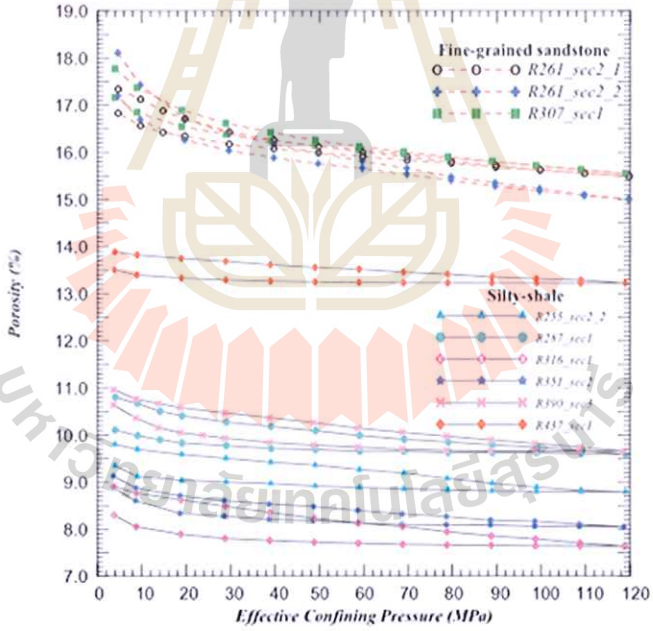

(b)

Figure 2.6 Stress dependent (a) permeability and (b) porosity of the sandstone and silty-shale for sandstone (red dashed lines) and silty-shale (solid black lines) (Dong et al., 2010).

reducing it back to 3 MPa. The permeability of the sandstone remained within a narrow range (10^{-14} to 10^{-13} m^2) shows in Figure 2.6. The permeability of the shale is more sensitive to the effective confining pressure (varying by two to three orders of magnitude) than the sandstone, possibly due to the existence of microcracks in the shale. Meanwhile, the sandstone and shale show a similar sensitivity of porosity to effective pressure, whereby porosity was reduced by about 10 to 20% when the confining pressure was increased from 3 to 120 MPa. The experimental results indicate that the fit of the models to the data points can be improved by using a power law instead of an exponential relationship (Figure 2.7).

Bloomfield and Williams (1995) observe the permeability from core analysis techniques of Permo-Triassic sandstones and shale from the Sherwood sandstone group of northern England by using gas and liquid measurements. Liquid permeability tests are performed using synthetic formation brines and deionized water. Gas permeability tests are used nitrogen as the permeant. Liquid permeability, k_l ranged from 9.0×10^{-19} m^2 to 2.4×10^{-12} m^2 and gas permeability, k_g ranged from 1.7×10^{-17} m^2 to 2.6×10^{-12} m^2. The liquid and gas permeability data exhibit log-normal frequency distributions; the log transformed liquid and gas permeability data have means of 5.1×10^{-16} m^2 and 4.3×10^{-5} m^2 respectively. A linear least-squares fit to the data has the form $\log_{10} k_l = 1.17\log_{10}k_g+1.51$. The ratios of k_l/k_g are ranging about 0.03 to 0.9.

Jones and Marathon (1988) present empirical equations that fit permeability and porosity data versus confining pressure. Each of these equations have four adjustable parameters. They also present a way to estimate the porosity and permeability at any pressure of interest between 0-10,000 psi by making only two measurements.

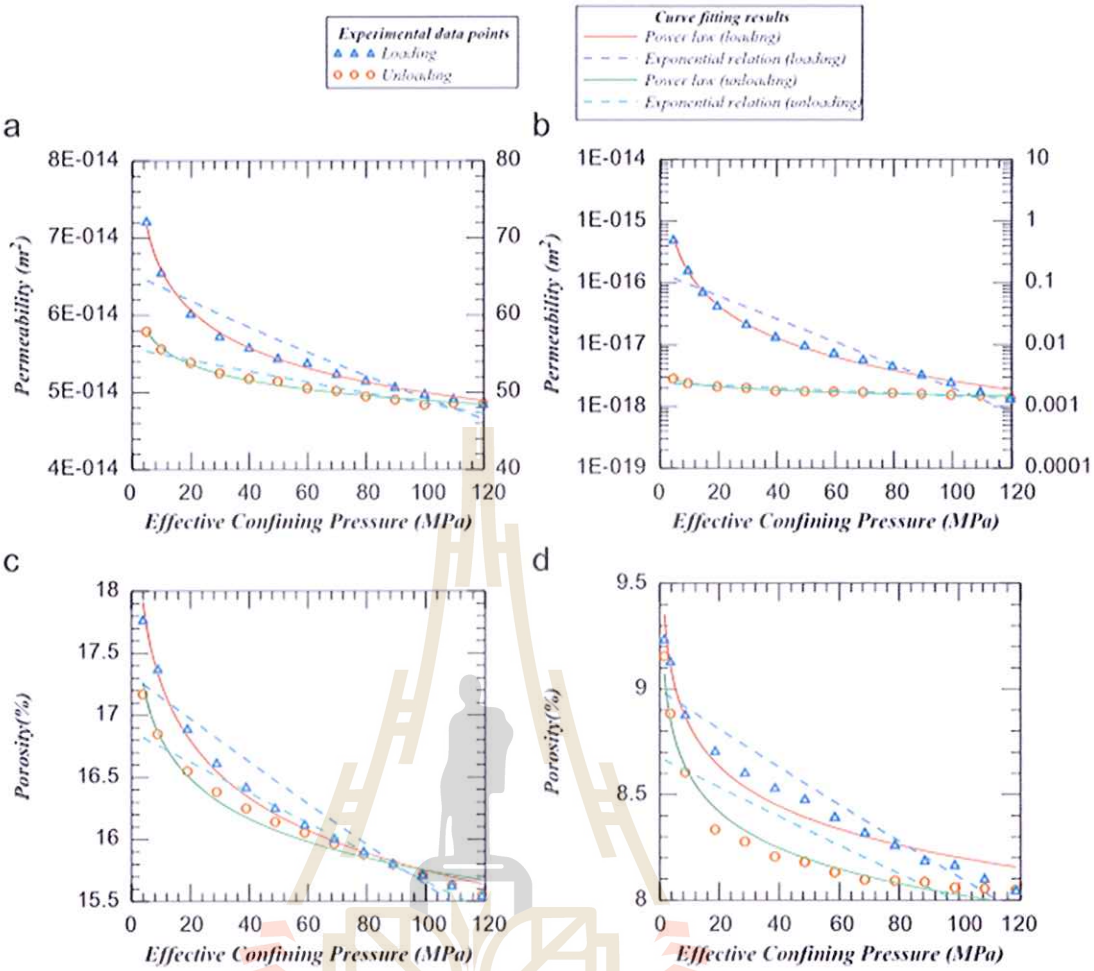

Figure 2.7 Loading and unloading curves of the stress dependent permeability and porosity for sandstone (a), (c) and silty-shale (b), (d) . Both an exponential relationship and a power law were utilized to fit the experimental data. (Dong et al., 2010)

Heiland et al. (2003) test triaxial permeability while controlling the axial strain and found that the permeability of marble decreases as the difference between axial pressure and confining pressure increases. Vairogs et al. (1971) suggest that changes in the effective stress affect the pore structure and skeletal structure of rocks, which affect the permeability of the rock. Additionally, many researchers construct the different mathematical models of permeability and confining pressure, including a cubic polynomial function, a logarithmic function, a power function, and other single-function mathematical models (Jennings et al., 1983 and Peng et al.,2003)

Mohiuddin et al. (2000) study the behavior of the stress-dependent porosity andpermeability of fifty Saudi Arabian reservoir rock samples. Half of the samples are sandstones, the other half limestones. The range of confining pressure is 0 to 82 MPa. Nine simultaneous measurements of porosity and permeability are taken in this range during loading, and four measurements during unloading to estimate the amount of hysteresis. The porosity-pressure curve for sandstones is convex from upward, and for limestone convex from downwards, as shown in Figure 2.8. In most of the sandstone samples the loss in porosity and permeability is regained during the downloading cycle, i.e. there is no appreciable hysteresis. This could be due to the fact that the pores are compressible and regained their original state after removing the pressure. It is essential to understand the stress-dependent porosity and permeability for reliable modeling of the reservoir during production, particularly for stress-sensitive reservoirs during large drawdowns. Most of the literature (Luffel, 1991; Davies and Holditch, 1998; Davies and Davies, 1999) are devoted to finding a relationship between porosity and permeability at in-situ conditions only.

Zhag et al. (2000) present a recently developed laboratory permeability test system capable of testing low permeability rocks either by using air as a permeant or by transient pulse method under high confining pressure conditions that simulate ground pressures at depths. The results of this study show that: 1) gas permeabilities of a dried rock specimen tested by air permeation are almost the same values as water permeabilities of the same saturated rock specimen is tested by the transient-pulse method. 2) the intrinsic permeabilities of Shirahama sandstone and Inada granite range from about 8.33×10^{-16} m^2 to 7.38×10^{-17} m^2 and from 1.86×10^{-17} m^2 to 6.94×10^{-20} m^2 respectively. They decrease monotonously with increasing the effective confining pressure, while the rate of decrease diminishes at higher confining pressure.

Zhang et al. (2016) investigate the porosity sensitive exponent are derived for several types of pore models. The results show that the magnitude of the porosity sensitive exponent depended on the geometry, scale and quantity of the matrix pores (circular pores and elliptical pores), as well as the fractures. A high porosity sensitive exponent induced a high stress sensitive coefficient. If the size of the fractures is similar to that of the matrix pores, the fracture could be treated as elliptical pores, and the porosity sensitive exponent ranged from 2 to 3. If the size of the fractures is considerably larger than matrix pores, the porosity sensitive exponent is much larger than 3.

Charukalas (1975) states that sandstones are important source of groundwater. It is necessary to understand their properties. One method to study the behavior of groundwater movement at depth in aquifers is through laboratory experiments. The results of experiments on the hydraulic conductivities of sandstones under a wide range of confining pressure are shown in Table 2.3 and Figure 2.9. Three upper Cretaceous

sandstone are used in the experiments; Mesa Verde and Middle Mancos sandstone from Carthage (Socorro County) and Point Lookout sandstone from San Juan Basin (McKinley County), New Mexico. Core sample approximately 1" diameter and 2.5" long, are placed between the upper and lower platen in the triaxial cell. Clamps and plastic jacket are used to prevent the confining oil from entering the core space. The initial confining pressure is 1000 psi in order to have enough sealing pressure between the plastic jacket and the core; this pressure increases by 1000 psi. The maximum confining pressure is 4000 psi, corresponding to overburden pressure of 4000 feet.

2.6 Effect of compaction on sandstone porosity

Compaction is a diagenetic process that begins on burial and may continue during burial to depths of 9 km (30,000 ft) or more. The compaction of sediments involves complex processes causing reduced porosity, increased density and other physical properties such as bulk modulus and velocity. Mechanical compaction processes are controlled by the effective stress and laboratory tests provide useful data on the mechanical compressibility of sediments with different mineralogical and textural compositions and fluid properties. Experimental compaction of artificial and natural samples provides valuable constraints on the mechanical compaction processes (Bjorlykke et al., 2008 and Wilson and Stanton, 1994). Generally, depth profiles of compacting sediments show an exponential decay in porosity with depth. Fine-grained sediments often show a reduction of porosity from 70% to 20% within the first 2 km of burial. Thereafter, porosity is lost at a much slower rate and can be approximated as a linear function of depth. In contrast, curves of sandstone porosity during burial show an approximately linear porosity loss throughout their entire history of burial.

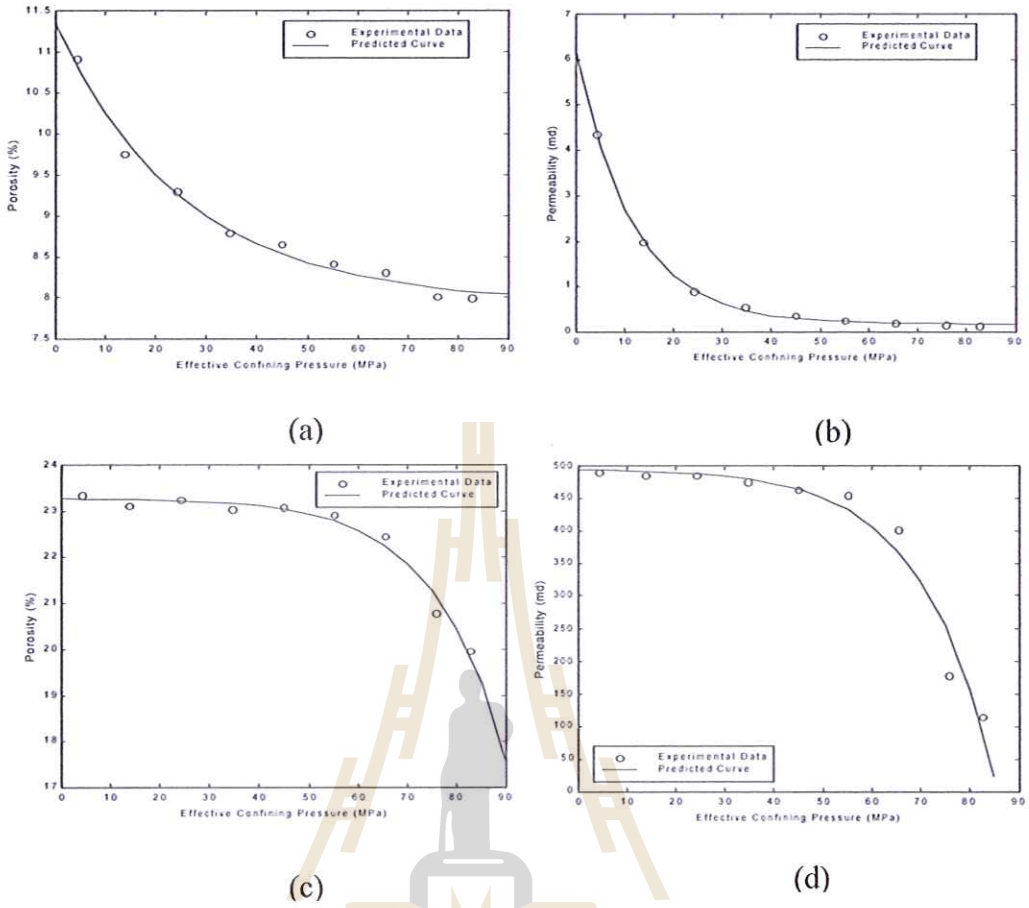

Figure 2.8 Porosity and permeability as a function effective confining pressure curve with curve fit for a representative reservoir sandstone samples (a), (b) and (c) and (d) for reservoir limestone samples (Mohiuddin et al., 2000).

Table 2.3 Summary of experimental results on other sandstones (Charukalas, 1975).

Rock	Hydraulic conductivity $\times 10^{-5}$ (m/s)				Original porosity (%)	New porosity (%)			
	Confining pressure (psi)								
	1000	2000	3000	4000		1000	2000	3000	4000
Mesa Verde	4	2.6	1.8	1.2	12	11.1	10.9	10.6	10.4
Middle Mancos	10.1	8.8	3.8	2.2	14	13.6	13.3	12.1	11.7
Point Lookout	0.00116	0.0008	0.0006	0.0004	19	17.8	17.6	17.4	16.9

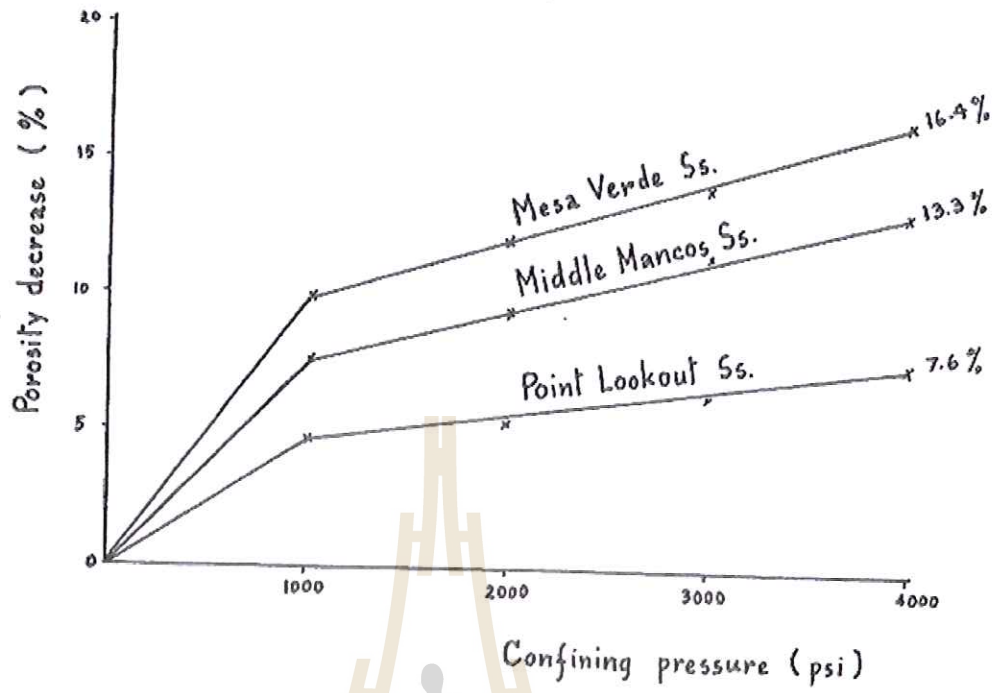

Figure 2.9 Confining pressure relate to porosity (Charukalas, 1975).

The extreme compaction of fine-grained siliciclastic rocks is of great importance to petroleum geologists, because if those rocks contain mobile petroleum hydrocarbons, those fluids are expelled upward into overlying porous rocks, which can then become petroleum reservoirs if they are capped by an appropriate seal.

2.7 Permeability and porosity relationship of rock

Correlations between porosity and permeability are often tested for sedimentary rocks in relation to petroleum geology and reservoir characterization. A general trend of increase in permeability with porosity can be expected. However, the effects of grain size, packing, compaction, and solution/dissolution processes related to development, preservation or loss of primary and secondary porosity can lead to a wide variety of relationships between permeability and various forms of porosity.

Permeability and porosity depend on pores in the rock. There are two discerned typologies of pores in rocks: closed and open pores. Closed pores are completely isolated from the external surface, not allowing the access of external fluids in either the liquid or gaseous phase. Closed pores influence parameters such as density and mechanical and thermal properties. Open pores are connected to the external surface and are therefore accessible to fluids, depending on the pore characteristics/size and the nature of fluid. Open pores can be further divided into dead-end or interconnected pores. The percentage of interconnected pores within the rock is known as effective porosity. Effective porosity excludes isolated pores and pore volume occupied by water adsorbedon clay minerals or other grains (Šperl Jan and Jiřina Trčková ,2008)

Luffel et al. (1991) derived an empirical relationship between core permeability and porosity at reservoir stress. Porosity and permeability were measured at ambient conditions and at reservoir stress for a large number of core samples from Travis peak tight sandstone gas reservoir. It was concluded that correlations are improved when applied to specific environmental rock types.

Davies and Holditch (1998) identify the main factor controlling stress-dependent permeability as pore geometry, in particular, the size and shape of the pore throat. They suggested an indirect way of estimating permeability in-situ, with the help of wireline logs. The logs would identify the rock type and using the correlations between porosity and permeability developed for different rock types, the in-situ permeability can be estimated.

Permeability and porosity depend on pores in the specimens. There are two discerned typologies of pores in rocks; closed and open pores. Closed pores are completely isolated from the external surface, not allowing the access of external fluids

in either the liquid or gaseous phase. Open pores are connected to the external surface and are therefore accessible to fluids, depending on the pore characteristics and the nature of fluid. The percentage of interconnected pores within the rock is known as effective porosity. Effective porosity excludes isolated pores and pore volume occupied by water adsorbed on clay minerals or other grains. As a result, only effective porosity can influence permeability because only open pores are interconnected and allow leaking water through (Šperl Jan and Jiřina Trčková , 2008; and Xuetao and Su Huang, 2017).

The changes in porosity due to deformation are controlled by alterations in grainsize and grain size distributions and by the production of microstructures which can modify pore connectivity. With decreasing in porosity can occur due to grain size rearrangement, confining pressure and cementation. The porosity decreases as the confining pressure increases due to pore space becomes to be compressed and grains increasingly compact. However, dissolved minerals, such as quartz, may also form new crystals in pore, which leads to a further decrease in porosity as described by Xuetao and Su Huang (2017).

2.8 Stress dependent specific storage

Dong et al (2010) study the specific storage as a function of effective confining pressure shown in Figure 2.7a and b, respectively. Clear differences exist between specific storage estimated using different stress dependent models of porosity. The specific storage calculated using an exponential relationship (Fig. 2.10a) ranged from 0.06×10^{-3} to 0.4×10^{-3} MPa^{-1} for the tested sandstone and shale when the confining pressure increase from 3 to 120 MPa. The specific storage calculated using a power

law (Fig. 2.10b) ranges from 2×10^{-3} to 0.2×10^{-3} for the sandstone. Generally, the estimated specific storage of the tested sedimentary rocks is reduced by about one order of magnitude.

Sharp and Domenico (1976) note that the specific storage of sediments is sharply reduced with increasing effective confining pressure. In other words, the specific storage of sediments should be highly dependent on the variation of effective confining pressure. It is thus suggested that a power law should be used to describe the stress dependent porosity when deriving the specific storage of the tested Pliocene to Pleistocene sedimentary rocks.

2.9 Permeability anisotropy

A sediment or sedimentary rock is defined to be anisotropic with respect to permeability when the magnitude of permeability at a given sample point changes with the direction of fluid flow through that sample. Permeability anisotropy in sediments is thought to be caused by the presence of grain-scale or layer-scale heterogeneities which have a preferred orientation (Lewis, 1988). Particularly in siliciclastic sands, singular grain-scale fabrics or mm to cm scale laminae, are commonly the result of discrete events of current deposition. Except in the case of coarse sands and gravels - with particle size > 0.5 mm, grain-scale fabrics are usually microscopic in nature. Bedding planes are distinguished from adjacent layers by particle size (e.g. coarse grains of quartz and very small clay particles), composition (e.g. feldspar versus mica), and color. The orientation of bedding plane in sands and sandstones typically ranges from sub-horizontal as produce from vertical aggradation of particles settling out of suspension, to surfaces inclined up to about 25 degrees from the horizontal, such as the

avalanche slopes of cross-bedded dunes. Flow or permeability anisotropy establish during deposition, may be further modified by burial diagenetic processes including compaction, dissolution and cementation of grains. If layering is horizontal, such structure will not only give rise to different horizontal permeabilities (k_h), but also a different vertical permeability (k_v) and the small-scale layered fabric is tilted from the horizontal, distinct horizontal permeabilities are referenced to that structure, that is, oriented either parallel or normal to the strike of inclined surfaces (Weber, 1982).

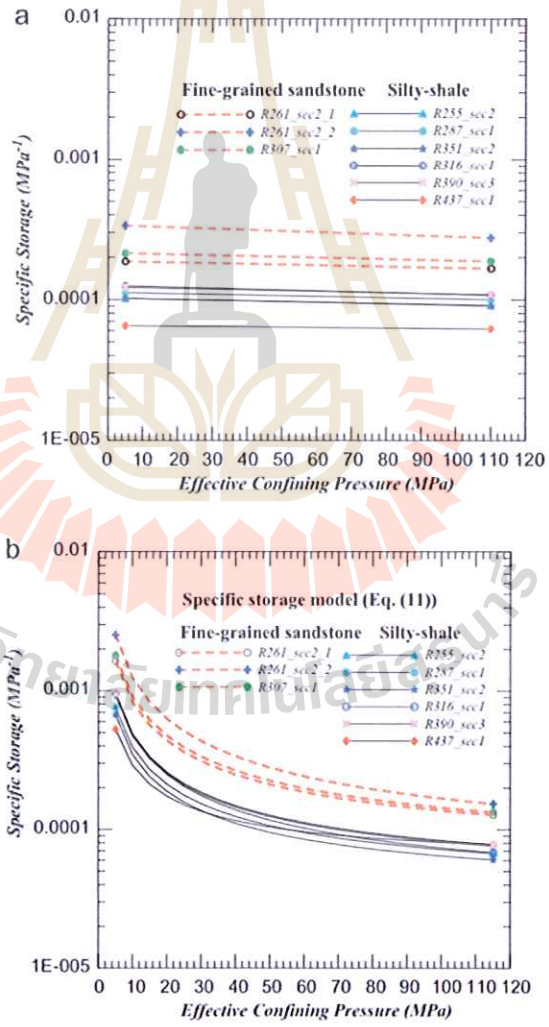

Figure 2.10 Stress dependent specific storage calculated based on an exponential relationship (a) and power law (b) (Dong et al ,2010).

Permeability anisotropy is commonly defined as the ratio of the coefficient of permeability parallel to the bedding plane, (k_h), to the coefficient of permeability in the direction normal to the bedding plane, (k_v). Therefore,

$$\text{Permeability Anisotropy} = k_h / k_v \tag{2.4}$$

As the required accuracy of permeability models increases, the need to account for anisotropy arises. Furthermore, the consideration of anisotropy is critical for processes where knowledge of the rate and direction of fluid movement is paramount, such as compression dewatering, contaminant transport, foundation settlement and hydrocarbon extraction. However, to date, knowledge of permeability anisotropy development resulting from the application of a compressive force to a deformable matrix of particles is incomplete. The anisotropic of rock permeability can be attributed to the arrangement direction of sand grains. In the deposition process, the long axis of sand is mainly parallel to the flow direction. The arrangement orientation of the rock matrix and the filling mode are closely linked to the direction of permeability. The permeability increases significantly in the parallel to the bedding planes and, is higher than that normal to the bedding planes as describe by Renner (2000) and Chen (2009).

2.10 Petrographic and classification of sandstones

The petrographic properties of sandstones provide a basic tool for its classification. Combine with other parameters it can be used to solve many intricate sedimentological problems. The composition of sandstone is influenced by the characteristics of provenance, the nature of sedimentary processes within the depositional basin, and kind of dispersed path that link provenance to depositional basin

(Dickinson and Suczek, 1979). Microtomographic (mCT) and thin section (TS) images are analyzed and compared regarding porosity and its distribution along the samples. The results show that mCT, although limited by its resolution, shows relevant information about the distribution of porosity and quantification of connected and non-connected pores. TS have no limitations concerning resolution but are limited by the experimental data and can only give information about connected pores. These two methods have their own advantages but when paired together they can make for a more complete analysis. TS for microscopic material investigation in transmitted and reflected light remain one of the most classic mineralogical methods of analysis in petrophysical research. TS provide an approach to identifying substances with relatively high spatial resolution. It allows an estimate of chemical compositions and provides clues for understanding the history of the rock formation. TS are made in the laboratory from the original samples from each group. They are cut in the middle of the sample with approximately 0.5 cm using a diamond saw, placed in a glass sheet and polished with abrasive powder until its thickness achieved 30 μm. After that, the thin section was viewed through a petrographic polarization microscope.

มหาวิทยาลัยเทคโนโลยีสุรนารี

CHAPTER III

SAMPLE PREPARATION

3.1 Introduction

This chapter describes the sample preparation to be used in the constant head flow test. The sandstone specimens selected for this research are from two sources: Phu Phan and Sao Khua formations. They belong to the Khorat group and widely expose in the northeast of Thailand.

3.2 Sample preparation

The selection criteria are that the rock should be homogeneous as much as possible. This is to minimize the intrinsic variability of the test results. Sample preparation has been carried out for series for constant head flow testing. It is conducted in the laboratory facility at the Suranaree University Technology. The process includes coring, cutting and grinding (Figures 3.1 and 3.2). Preparation of these samples follows the ASTM standard (ASTM D4543-08) with nominal dimensions of 5.4 cm in diameter and 8.1 cm in length. Tables 3.1 to 3.3 give a summary of sandstone specimen dimensions. The ratio of specimen length to diam eter (L/D) is about 1.5. A minimum of ten specimens are prepared for each rock type, as shown in Figures 3.3 to 3.6. The rock specimens are submerged under water in vacuum chamber until its weight becomes unchanged at negative pressure of 0.1 MPa, which takes about 48 hours for determine effective porosity and note weight every 1 hour unit 48 hours (Figure 3.7). The Phu Phan specimens have average water contents ($w_{ave.}$) of 3.37% and 3.31%.

(Figure 3.8 and 3.9). Table 3.4 shows water contents of the specimen under saturated conditions. The specimen density is averaged as 2.42 ± 0.02 g/cc for Phu Phan sandstone, and 2.36 ± 0.02 g/cc for Sao Khua sandstone.

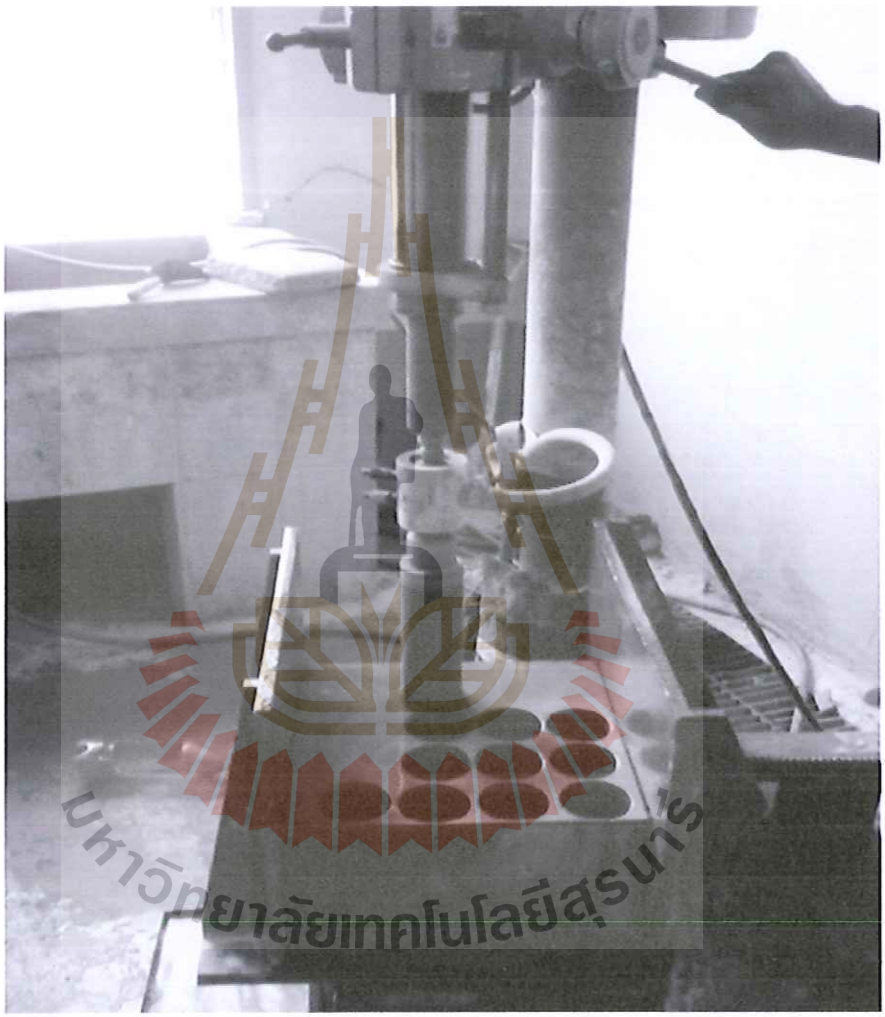

Figure 3.1 Laboratory core drilling. Core drilling machine (model SBEL 1150) used to prepare core specimens using diamond impregnated bit with diameter of 54 mm.

มหาวิทยาลัยเทคโนโลยีสุรนารี

Figure 3.2 Core specimen cut to length by a cutting machine.

Table 3.1 Specimens with bedding planes parallel to main axis.

Rock Type	Specimen Number	Weight (g)	Average Diameter (mm)	Average Length (mm)	Density (g/cc)
Phu Phan Sandstone	PP-01	458.76	53.60	84.00	2.42
	PP-02	421.39	53.70	77.50	2.40
	PP-03	454.25	53.60	83.20	2.42
	PP-04	448.00	53.70	82.70	2.44
	PP-05	454.00	53.70	82.20	2.42
Sao Khua Sandstone	SK-01	443.44	53.40	83.60	2.37
	SK-02	445.84	53.70	83.60	2.35
	SK-03	426.52	53.70	79.70	2.36
	SK-04	447.37	53.64	83.34	2.38
	SK-05	442.24	53.80	83.20	2.34

มหาวิทยาลัยเทคโนโลยีสุรนารี

Table 3.2 Specimens for Phu Phan sandstone with core axis normal to bedding plane.

Rock Type	Specimen Number	Weight (g)	Average Diameter (mm)	Average Length (mm)	Density (g/cc)
Phu Phan Sandstone	PP-06	446.74	53.20	83.40	2.41
	PP-07	451.21	53.30	82.40	2.45
	PP-08	446.43	53.20	83.70	2.40
	PP-09	444.64	53.70	81.60	2.41
	PP-10	444.24	53.30	82.40	2.42

Table 3.3 Specimens for Sao Khua sandstone with core axis normal to bedding plane.

Rock Type	Specimen Number	Weight (g)	Average Diameter (mm)	Average Length (mm)	Density (g/cc)
Sao Khua Sandstone	SK-06	433.52	54.20	81.30	2.31
	SK-07	455.14	54.10	83.60	2.37
	SK-08	452.71	53.60	84.40	2.38
	SK-09	434.23	54.24	80.40	2.34
	SK-10	434.00	53.80	81.14	2.35

มหาวิทยาลัยเทคโนโลยีสุรนารี

Figure 3.3 Phu Phan sandstone specimens with core axis parallel bedding plane.

Figure 3.4 Sao Khua sandstone specimens with core axis parallel bedding plane.

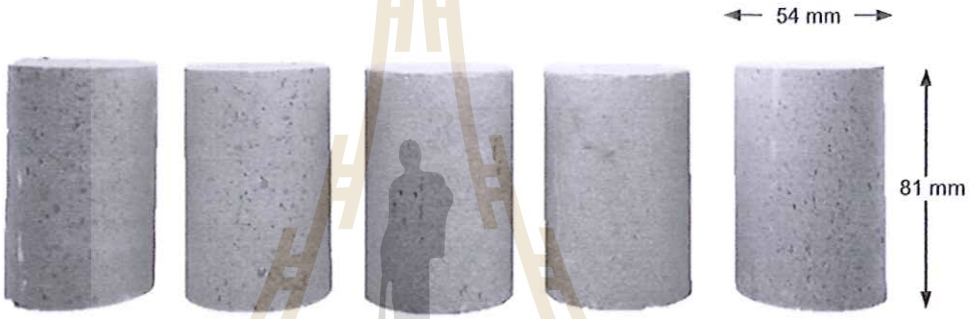

Figure 3.5 Phu Phan sandstone specimens with core axis normal to bedding plane.

Figure 3.6 Sao Khua sandstone specimens with core axis normal to bedding plane.

มหาวิทยาลัยเทคโนโลยีสุรนารี

Figure 3.7 Rock specimens saturated in vacuum-chamber at a negative pressure of 0.1 MPa for 48 hours.

มหาวิทยาลัยเทคโนโลยีสุรนารี

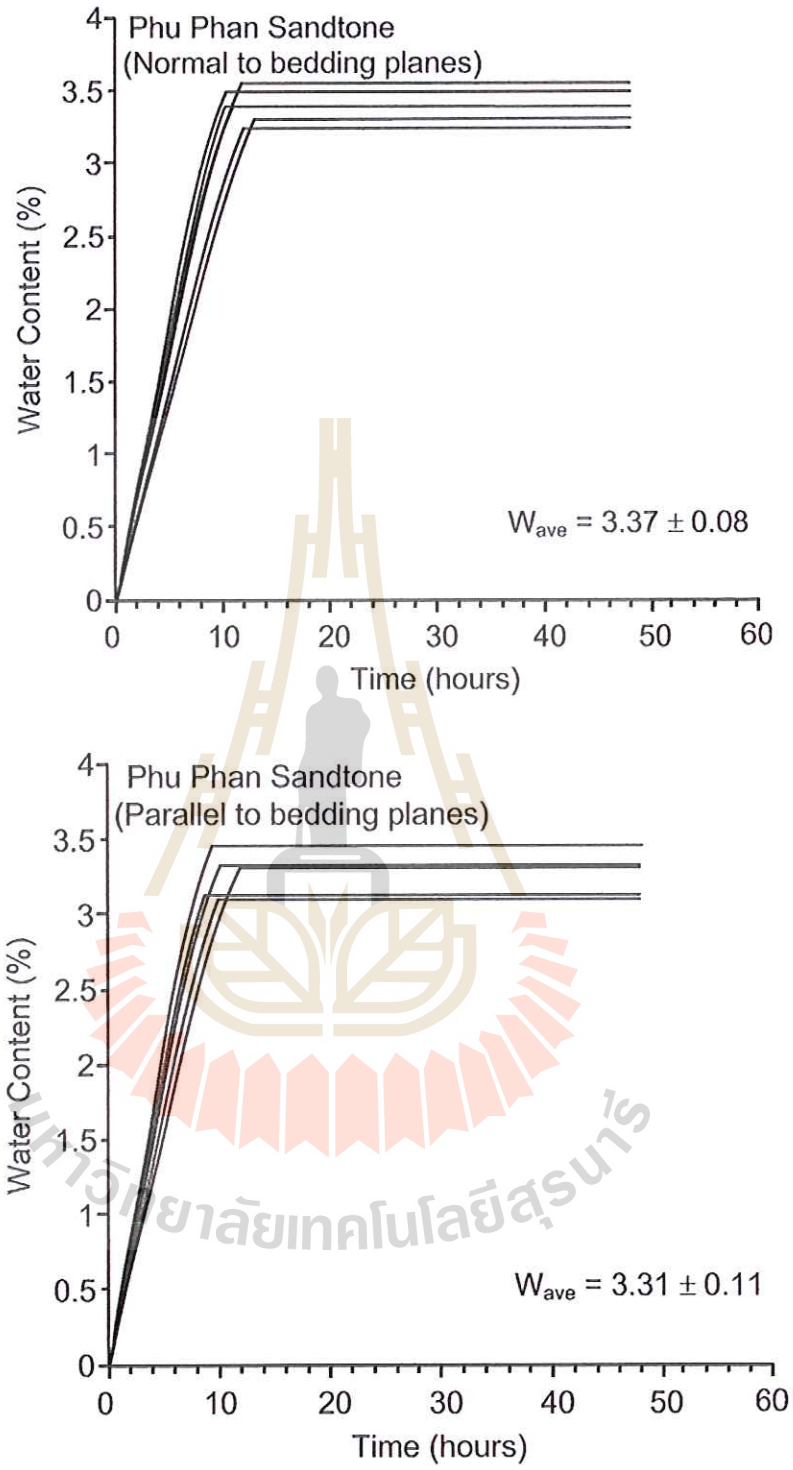

Figure 3.8 Water contents of Phu Phan sandstone specimens as a function of time.

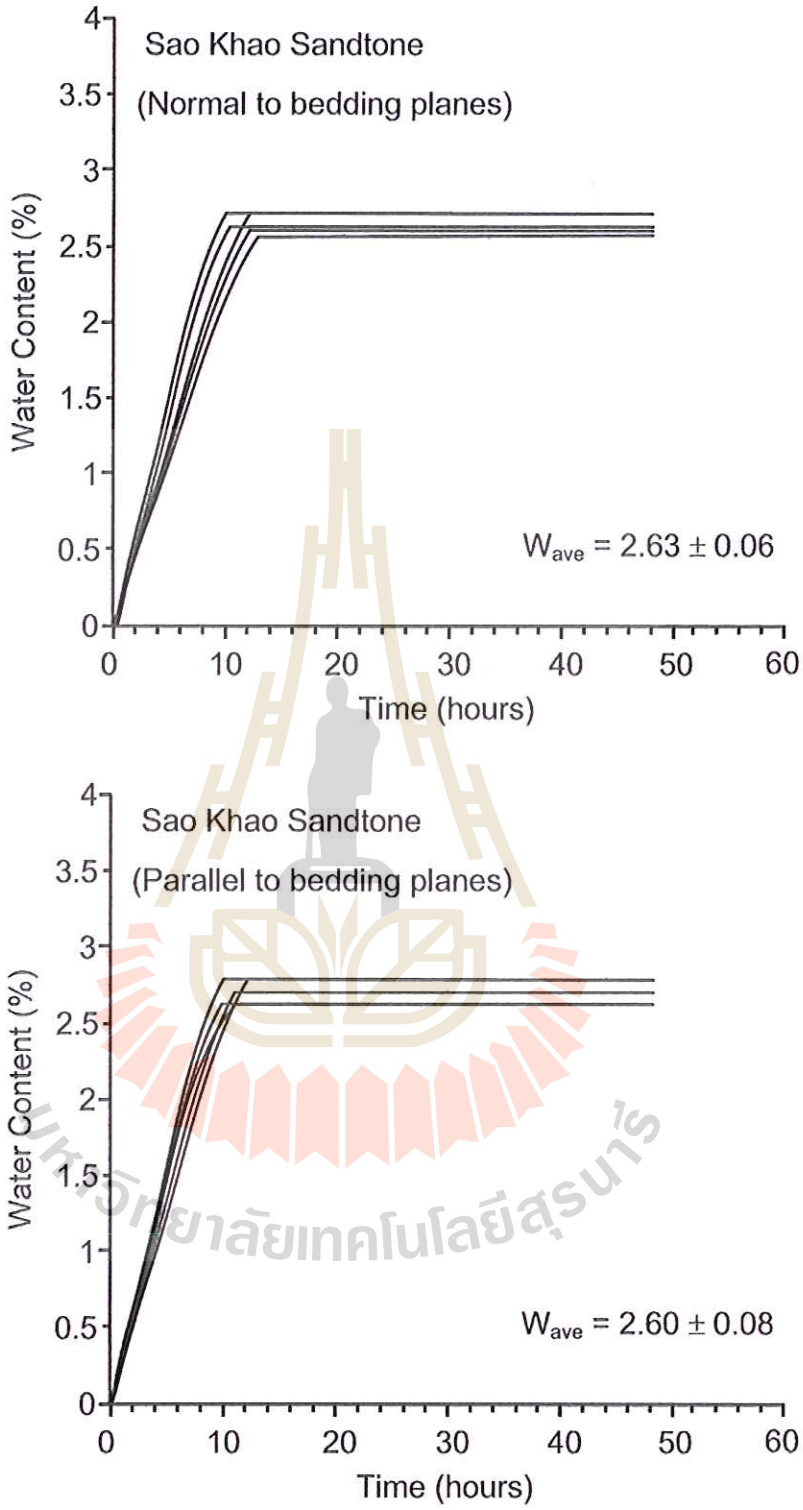

Figure 3.9 Water contents of Sao Khua sandstone specimens as a function of time.

Table 3.4 Saturated sandstone specimens.

Rock Type	Specimen Number	Wet Weight (g)	Wet Density (g/cc)	Water content (%)
Phu Phan Sandstone	PP-01	474.00	2.50	3.32
	PP-02	435.40	2.48	3.32
	PP-03	470.00	2.50	3.47
	PP-04	462.10	2.47	3.13
	PP-05	469.20	2.52	3.31
	PP-06	462.61	2.43	3.41
	PP-07	466.22	2.46	3.28
	PP-08	457.50	2.53	3.49
	PP-09	456/52	2.42	3.27
	PP-10	457.13	2.42	3.38
Sao Khua Sandstone	SK-01	455.33	2.39	2.68
	SK-02	457.24	2.41	2.56
	SK-03	437.22	2.42	2.51
	SK-04	459.37	2.43	2.68
	SK-05	453.31	2.40	2.50
	SK-06	445.24	2.37	2.70
	SK-07	467.44	2.43	2.70
	SK-08	464.61	2.44	2.63
	SK-09	445.30	2.40	2.55
	SK-10	445.12	2.41	2.56

มหาวิทยาลัยเทคโนโลยีสุรนารี

3.3 Thin section

Petrographic examinations are made for following purposes: (1) minerals identification, (2) shape and grain size of minerals, (3) pore distribution and (4) sorting. Four thin-sections are made, two thin-sections are parallel to bedding planes and two thin-sections are perpendicular to bedding planes. The thin section preparations are carried out by using high-speed saw, as shown in Figure 3.9. Example of thin-sections for petrographic analysis are shown in Figure 3.10.

Figure 3.10 Cut-off to the slide by using thin section saw.

มหาวิทยาลัยเทคโนโลยีสุรนารี

3.4 Petrographic analysis

The Phu Phan sandstone is composed mainly of quartz and iron-oxides and can be classified as quartz arenite. Grains are larger than those of Sao Khua and are subangular to subrounded with moderate sphericity. Shapes of interstitial pore are subangular to subrounded with average porosity ranging from 5-10% (Table 3.5). The Sao Khua sandstone is consisted of quartz, feldspar, mica, rock fragments and iron oxides; thus, classified as feldspathic greywacke. Grains are angular-subangular and low sphericity, interstitial pores are angulated and elongated. Average porosity as observed in the photomicrographs is <3% (Table 3.6).

Figure 3.11 Thin section slides of Phu Phan and Sao Khua sandstones in directions normal (a),(c) and parallel (b),(d) to bedding planes.

มหาวิทยาลัยเทคโนโลยีสุรนารี

Table 3.5 Summary of petrographic analysis.

Rock Type	Directions	Photomicrograph	Photographic description
Phu Phan Sandstone	Normal to bedding planes	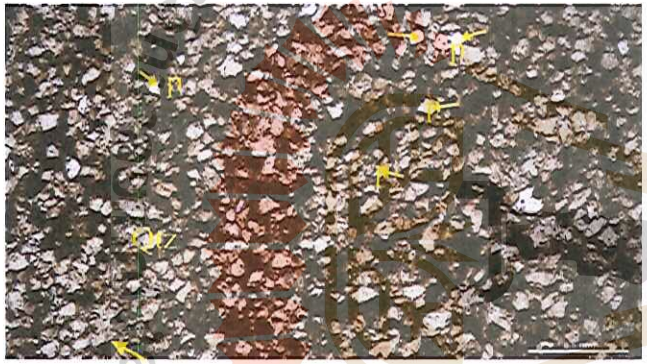	**Minerals identification:** 90% Quartz (0.2-0.8 mm) and 10% other (0.5-1 mm) **Shape and grain size:** subangular to subrounded **Interstitial pores:** subangular to subrounded **Sorting:** well sorted **Description:** Fine grained sandstone, brownish yellow, Brownish yellow color may originate from limonite. Remark *P= Pore space, Qtz= Quartz Fsp= Feldspar
	Parallel to bedding planes		

Table 3.6 Summary of petrographic analysis (continued).

Rock Type	Directions	Photomicrograph	Photographic description
Sao Khua Sandstone	Normal to bedding planes		**Minerals identification:** 70% Feldspar (0.1-0.5 mm) 20% quartz (0.1-0.5 mm) 5% mica (0.1-0.2 mm) 3% rock fragment (0.1-0.3 mm), and 2% iron oxides (0.1-0.3 mm) **Shape and grain size:** angular-subangular **Interstitial pores:** angulated and elongated **Sorting:** moderately sorted **Description:** Fine grained sandstone and red color may point to occurrence of oxidization by Fe-oxide
	Parallel to bedding planes		

CHAPTER IV

TESTING METHODS AND RESULTS

4.1 Introduction

The objective of this chapter is to describe the flow testing of effective porosity of Phu Phan and Sao Khua sandstone specimens under different confining pressures. The flow directions are normal and parallel to the bedding planes. Anisotropic permeability is determined. Since the fracture permeability is not considered here, the findings can be useful for a conservative prediction of the yield pumping rates of the two sandstone formations.

4.2 Test apparatus and method

Figures 4.1 and 4.2 show the test arrangement. Before testing, the specimens are oven dried at 100 °C, and saturated in a vacuum-chamber at negative pressure of 0.1 MPa for 48 hours. The specimen is then placed in a triaxial cell which is used to inject water pressure under constant confining pressure. The confining pressures are from 10 to 50 MPa. The injected water pressure is about 0.69 MPa, which is controlled by a regulating valve connected on the nitrogen gas tank. The outlet pressure is taken as the atmospheric pressure, and is assumed to be 1 atm. Pipette with precision of 0.1 cc and 0.01 cc is used to collect the outflow of water for high and low flow rates, respectively. The flow rates under each confining pressure are measured to calculate the rock permeability and porosity. Testing durations are up to 19 to 46 days.

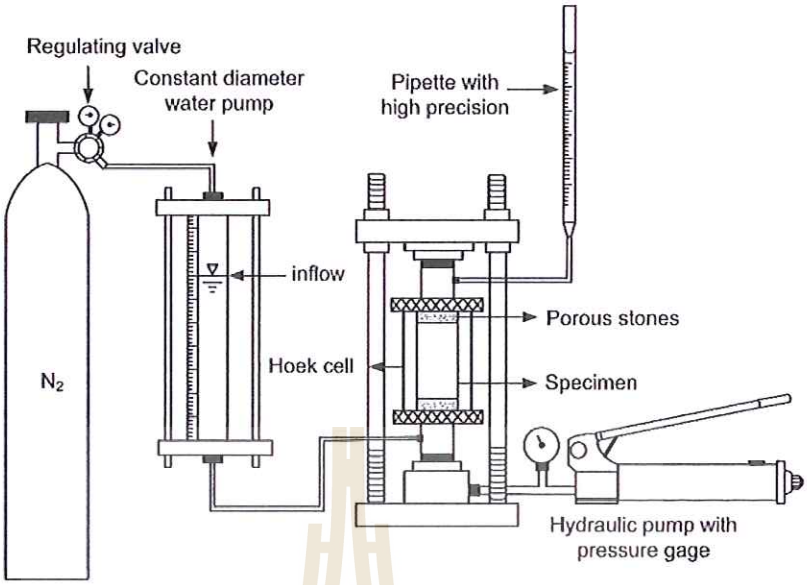

Figure 4.1 Laboratory arrangement scheme for constant head flow test under high confining pressures.

Figure 4.2 Laboratory setup for constant head flow test under high confining pressures.

4.3 Test results

The flow rates (Q) as a function of time for all specimens are shown in Figures 4.3 to 4.22 and in Table 4.1. The curves show inflow and outflow with the flow directions parallel and normal to bedding planes. The flow rates are measured as a function of time until the inflow and outflow rates are equal. This is to ensure that the specimens are under saturated condition, and that the mass balance flow rates are reached. The results indicate that the outflow rate increases with times and decreases with increasing confining pressures. The time at which the inflow and outflow rates are balanced increases with increasing confining pressures. For both sandstone types, the flow rates normal to the bedding plane are lower than those parallel to the bedding plane. The Phu Phan sandstone gives the flow rate higher than that of Sao Khua sandstone for both normal and parallel to the bedding planes. This is probably controlled by the porosity and pore space arrangement of the specimens.

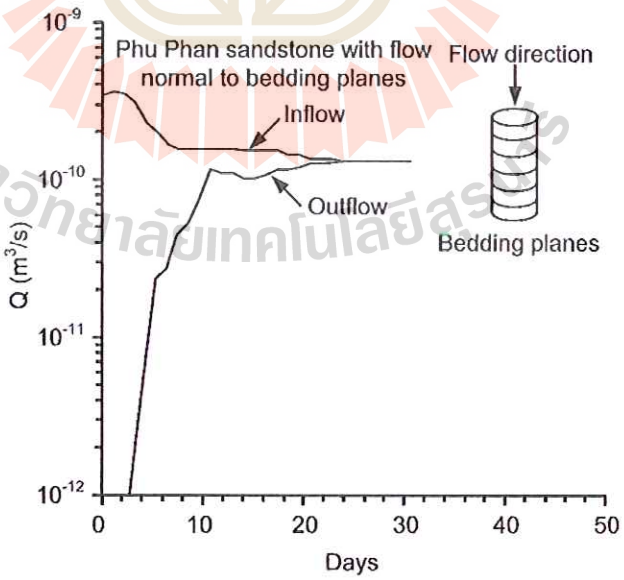

Figure 4.3 Flow rates normal to bedding planes as a function of time for confining pressures at 10 MPa for Phu Phan sandstone.

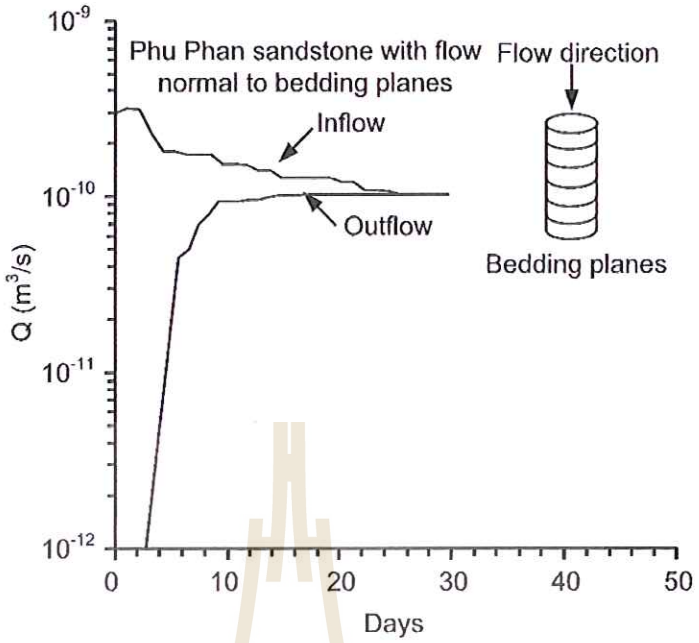

Figure 4.4 Flow rates normal to bedding planes as a function of time for confining pressures at 20 MPa for Phu Phan sandstone.

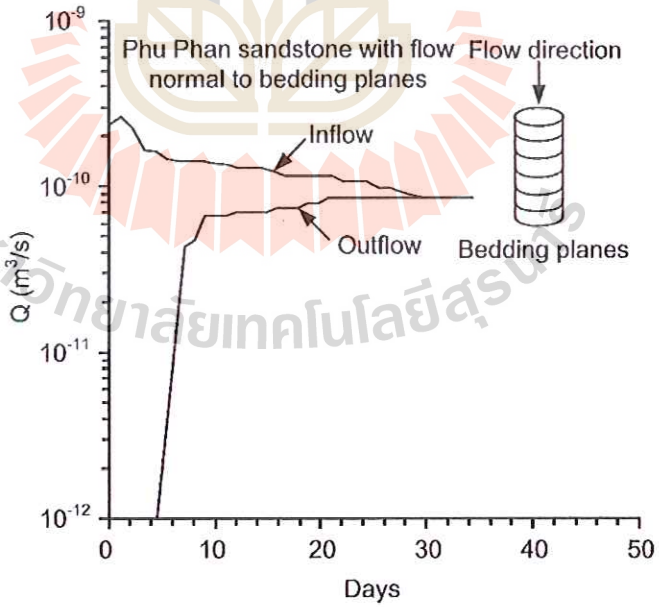

Figure 4.5 Flow rates normal to bedding planes as a function of time for confining pressures at 30 MPa for Phu Phan sandstone.

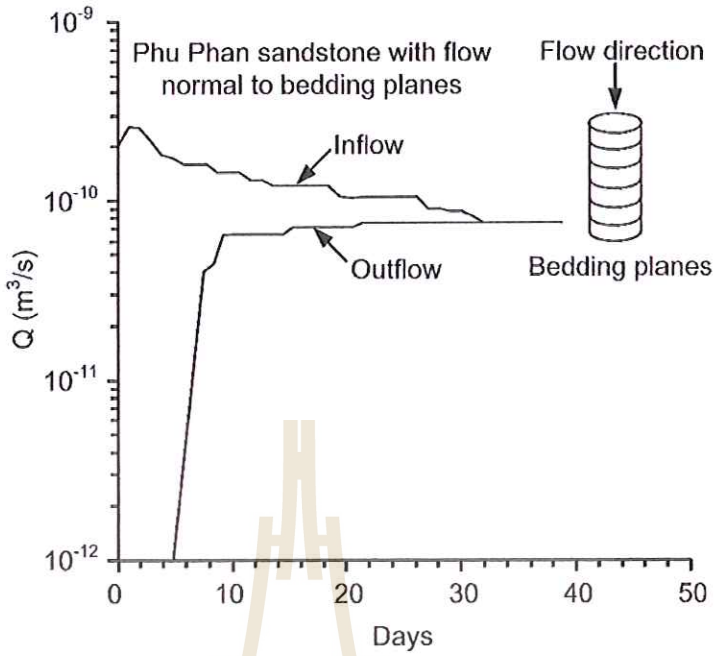

Figure 4.6 Flow rates normal to bedding planes as a function of time for confining pressures at 40 MPa for Phu Phan sandstone.

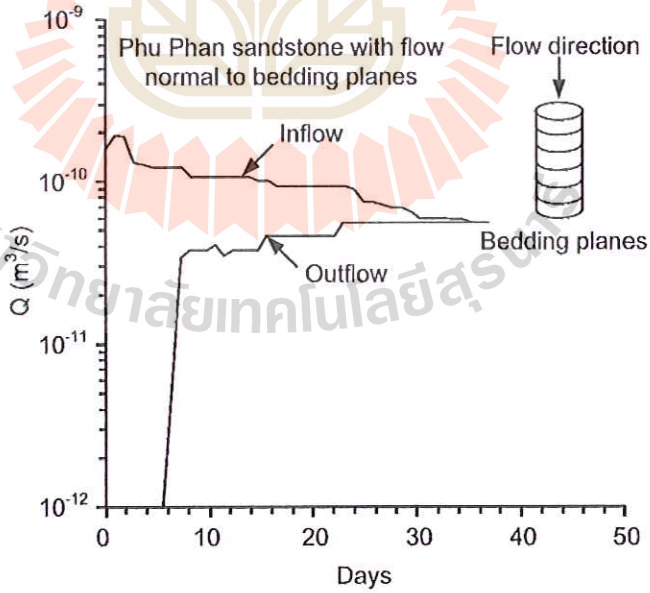

Figure 4.7 Flow rates normal to bedding planes as a function of time for confining pressures at 50 MPa for Phu Phan sandstone.

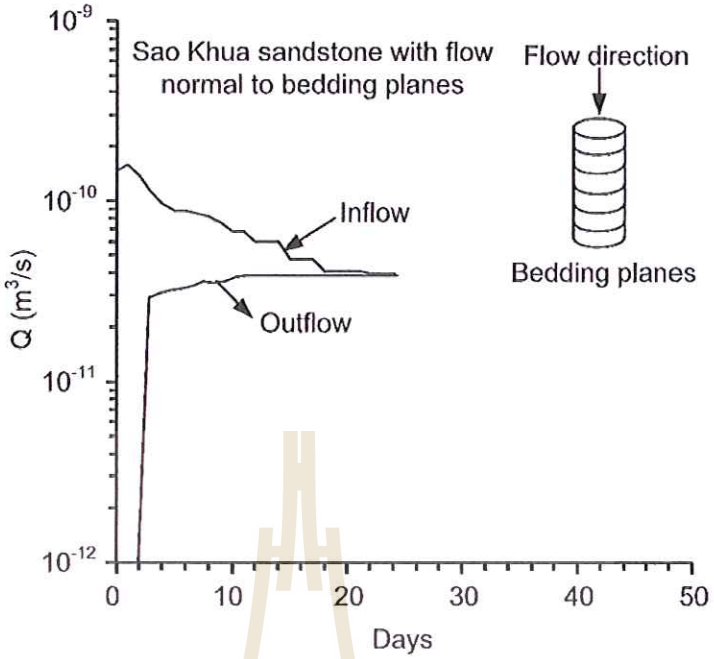

Figure 4.8 Flow rates normal to bedding planes as a function of time for confining pressures at 10 MPa for Sao Khua sandstone.

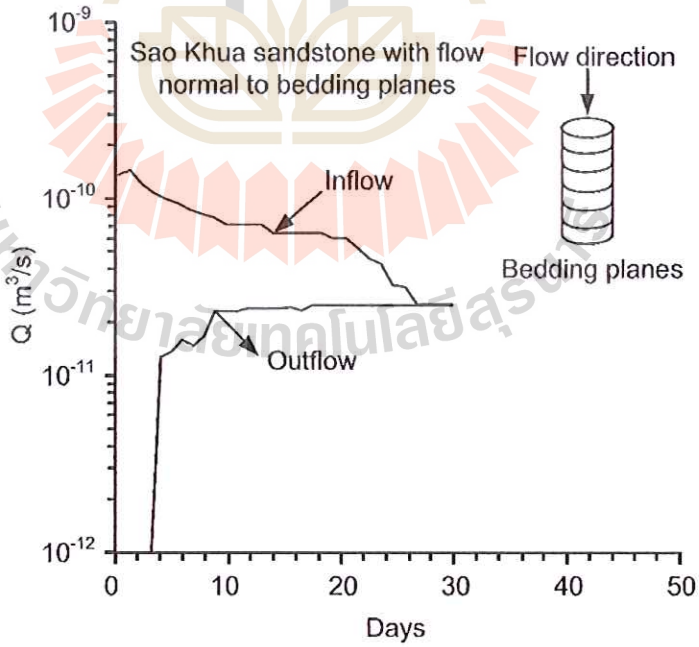

Figure 4.9 Flow rates normal to bedding planes as a function of time for confining pressures at 20 MPa for Sao Khua sandstone.

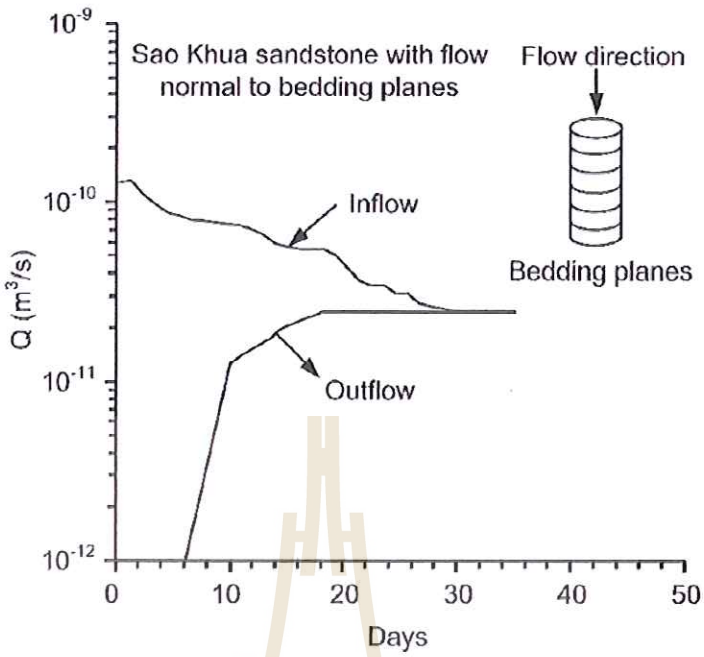

Figure 4.10 Flow rates normal to bedding planes as a function of time for confining pressures at 30 MPa for Sao Khua sandstone.

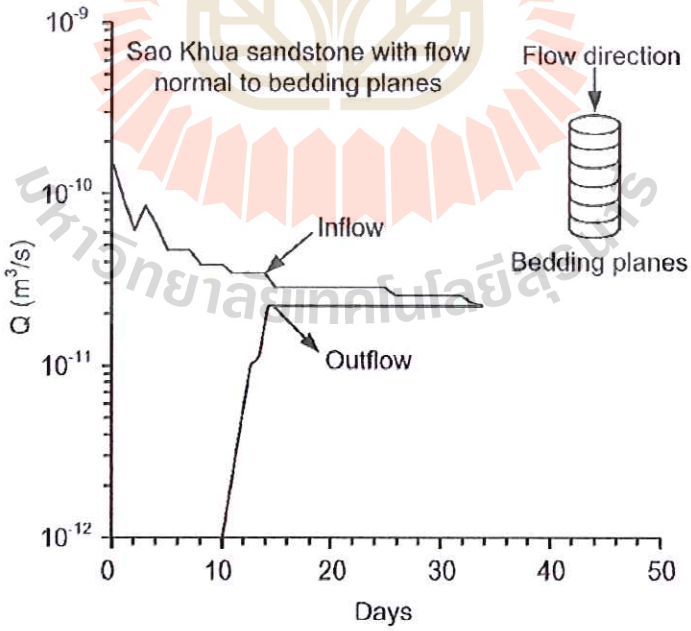

Figure 4.11 Flow rates normal to bedding planes as a function of time for confining pressures at 40 MPa for Sao Khua sandstone.

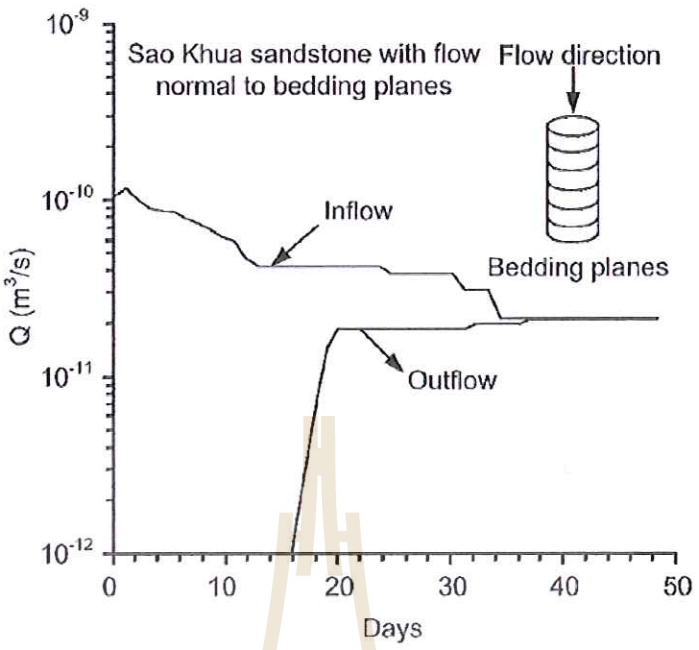

Figure 4.12 Flow rates normal to bedding planes as a function of time for confining pressures at 50 MPa for Sao Khua sandstone.

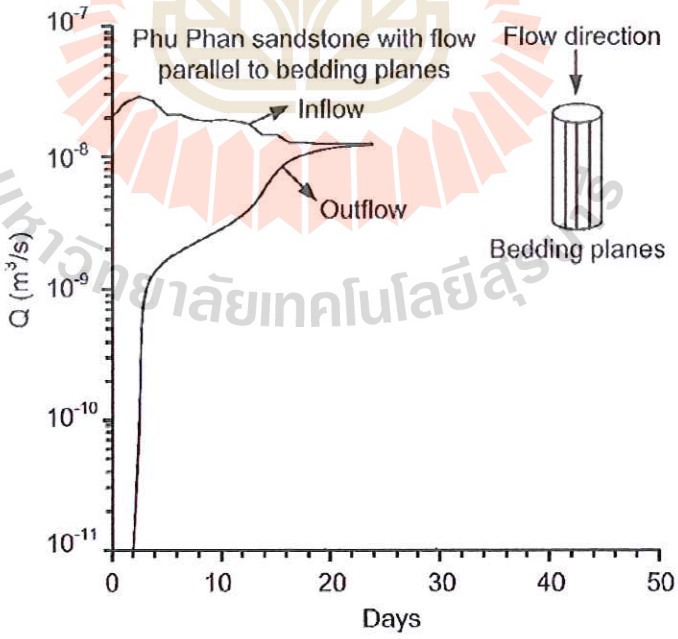

Figure 4.13 Flow rates parallel to bedding planes as a function of time for confining pressures at 10 MPa for Phu Phan sandstone.

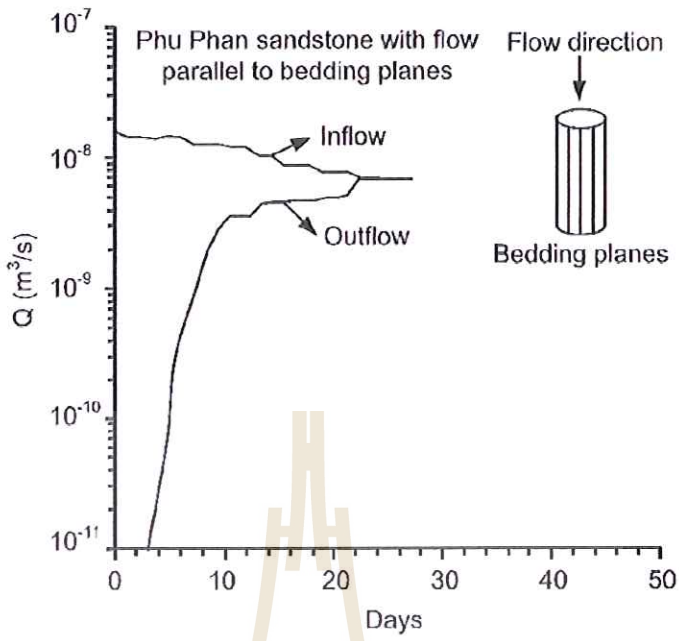

Figure 4.14 Flow rates parallel to bedding planes as a function of time for confining pressures at 20 MPa for Phu Phan sandstone.

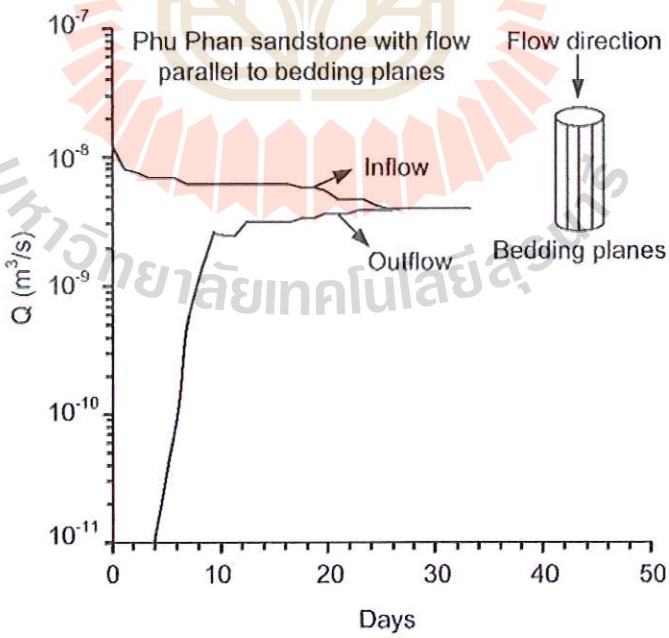

Figure 4.15 Flow rates parallel to bedding planes as a function of time for confining pressures at 30 MPa for Phu Phan sandstone.

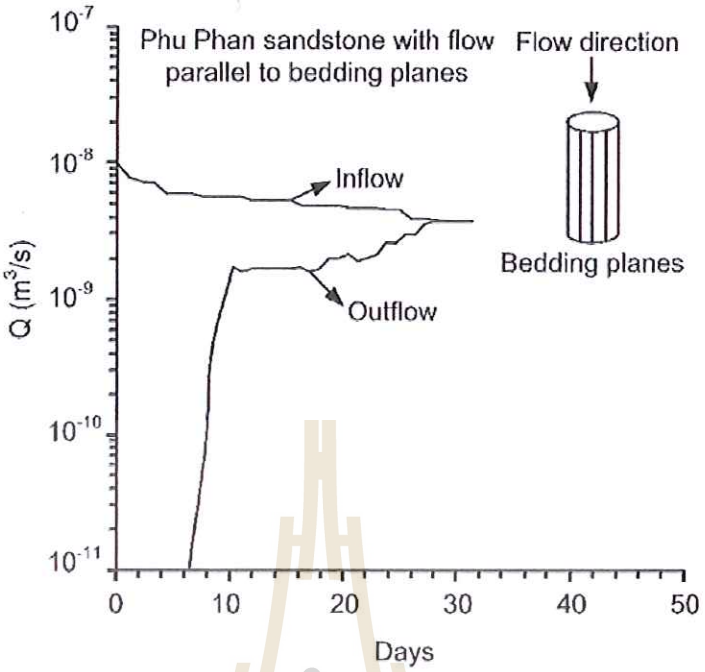

Figure 4.16 Flow rates parallel to bedding planes as a function of time for confining pressures at 40 MPa for Phu Phan sandstone.

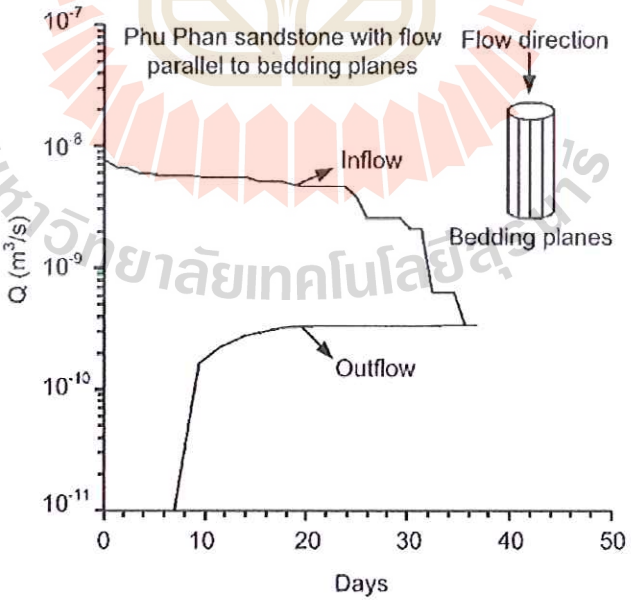

Figure 4.17 Flow rates parallel to bedding planes as a function of time for confining pressures at 50 MPa for Phu Phan sandstone.

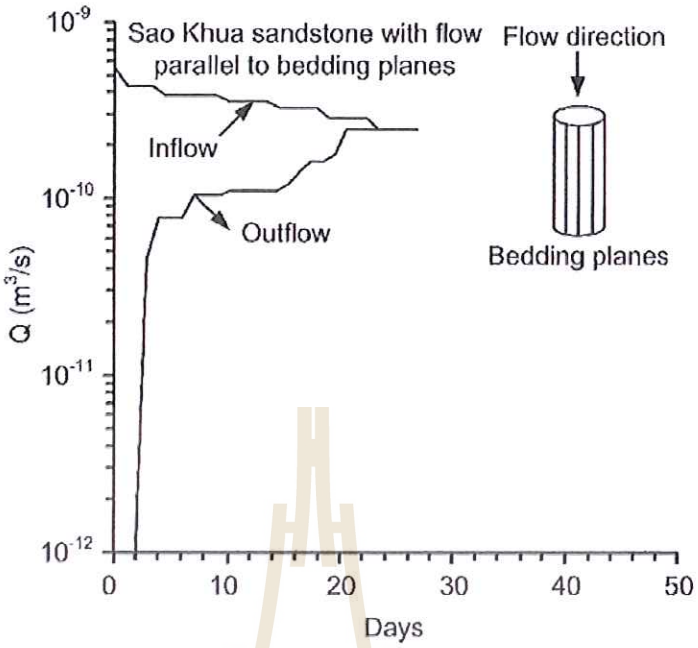

Figure 4.18 Flow rates parallel to bedding planes as a function of time for confining pressures at 10 MPa for Sao Khua sandstone.

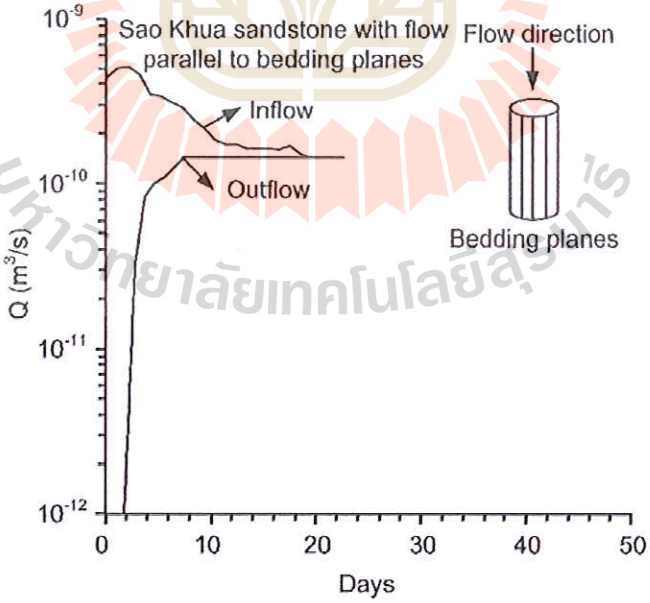

Figure 4.19 Flow rates parallel to bedding planes as a function of time for confining pressures at 20 MPa for Sao Khua sandstone.

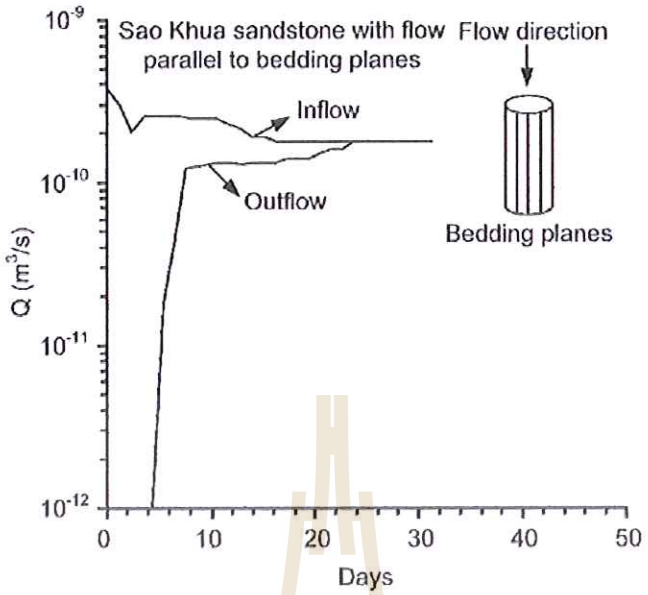

Figure 4.20 Flow rates parallel to bedding planes as a function of time for confining pressures at 30 MPa for Sao Khua sandstone.

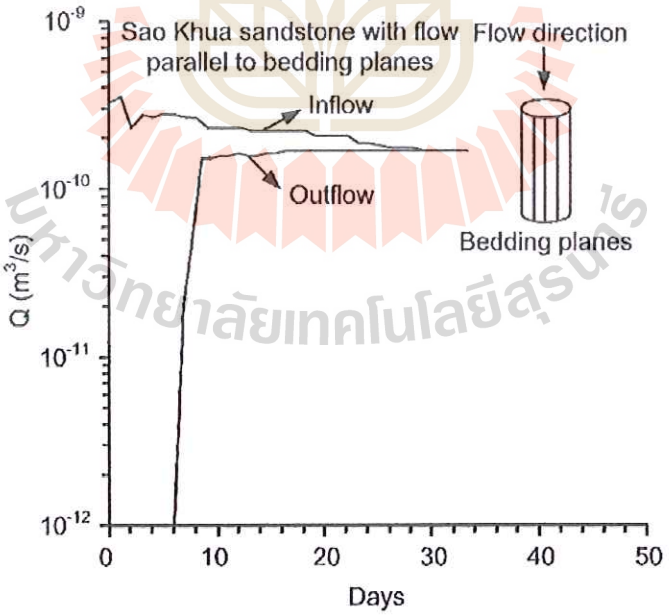

Figure 4.21 Flow rates parallel to bedding planes as a function of time for confining pressures at 40 MPa for Sao Khua sandstone.

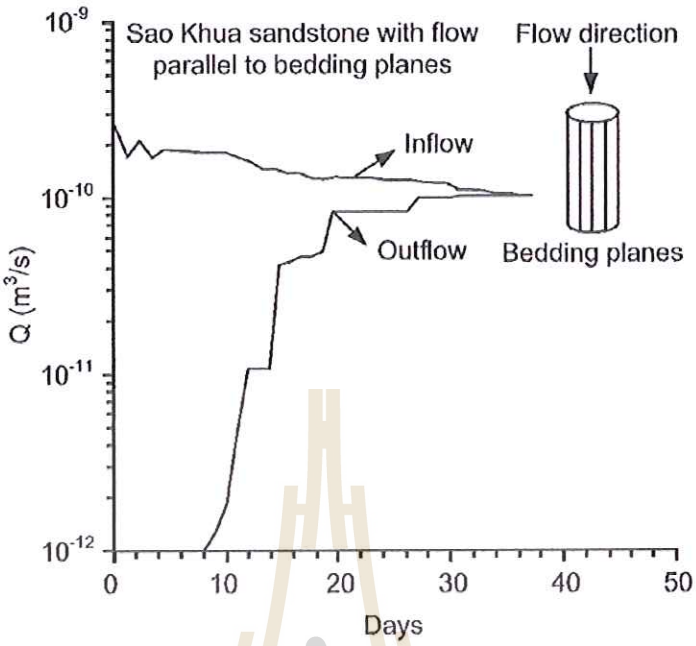

Figure 4.22 Flow rates parallel to bedding planes as a function of time for confining pressures at 50 MPa for Sao Khua sandstone.

มหาวิทยาลัยเทคโนโลยีสุรนารี

Table 4.1 Summary of test results.

Rock Type	Flow Directions	Confining Pressures (MPa)	Testing Time (Days)	Flow Rates (cc/hour)
Phu Phan sandstone	Parallel (//)	10	19	29.05
		20	24	9.79
		30	26	5.76
		40	30	4.61
		50	35	2.81
	Normal (⊥)	10	24	3.46
		20	27	1.66
		30	30	0.58
		40	34	0.43
		50	37	0.22
Sao Khua sandstone	Parallel (//)	10	22	14.40
		20	27	5.00
		30	30	2.81
		40	34	1.58
		50	37	0.65
	Normal (⊥)	10	24	0.68
		20	26	0.40
		30	29	0.14
		40	35	0.07
		50	46	0.04

4.4 Permeability Calculation

The hydraulic conductivity (K_{hc}) can be calculated from the test results. Based on the Darcy's law (Indraratna and Ranjith, 2001) the conductivity for one-dimensional flow can be calculated from:

$$K_{hc} = Q / A(\Delta h/L) \tag{4.1}$$

where K_{hc} is hydraulic conductivity (m/s), Q is flow rate (m^3/s), A is a cross-section area of flow (m^2), γ_w is unit weight of water (9,789 N/m^3), and $\Delta h/L$ is hydraulic head gradient. The hydraulic conductivity can be used to calculate the intrinsic permeability (k) as:

$$k = (K_{hc}\,\mu/\gamma_w) \tag{4.2}$$

where μ is dynamic viscosity of water (1.005×10^{-3} N·s/m^2). The intrinsic permeability values parallel and normal to the bedding planes are plotted as a function of confining pressure in Figure 4.23. The results show that the intrinsic permeability decreases when confining pressures increase from 10 to 50 MPa. The intrinsic permeability of Phu Phan sandstone is higher than that of Sao Khua sandstone for all test conditions. The permeability of rock specimens with flow direction parallel to the bedding planes are always greater than those normal to the bedding planes. Table 4.2 shows the empirical equation and parameters used to fit the curve in Figure 4.23. The parameter k_0 represents the rock permeability under zero confinement.

4.5 Effective Porosity Calculation

The effective porosity of the two sandstones can also be determined from the specimens tested under each confining pressure. This can be done by weighting the specimens before and after placing in an oven for 24 hours after flow testing. The weight differences represent the weight of water. The effective porosity can then be calculated by (ASTM C830):

$$n_e = [(W - d)/\rho_w]/V) \times 100 \tag{4.3}$$

where W is saturated weight of specimen (g), d is dry weight of specimen (g), ρ_w is density of water (g/cm^3) and V is total bulk volume of specimen (cm^3). The results indicate that the effective porosity of sandstones in the flow direction normal and parallel to the bedding plane are equal, that its controlled by alterations in grain size

and distributions and by the production of microstructures which can modify pore connectivity. With decreasing in porosity can occur due to grain size rearrangement, confining pressure and cementation. and decrease with increasing confining pressures (Figure 4.24). The porosity of Phu Phan sandstone is higher than that of Sao Khua sandstone, particularly under high confining pressures. They are ranging from 4.5% to 7.3% for Phu Phan sandstone and 1.9% to 4.3% for Sao Khua sandstone. The reductions of the specimen diameters and lengths have been measured after they are removed from the confining chamber. It is found that diameters and lengths reduce as increasing the confining pressure as shown in Table 4.3 to 4.6.

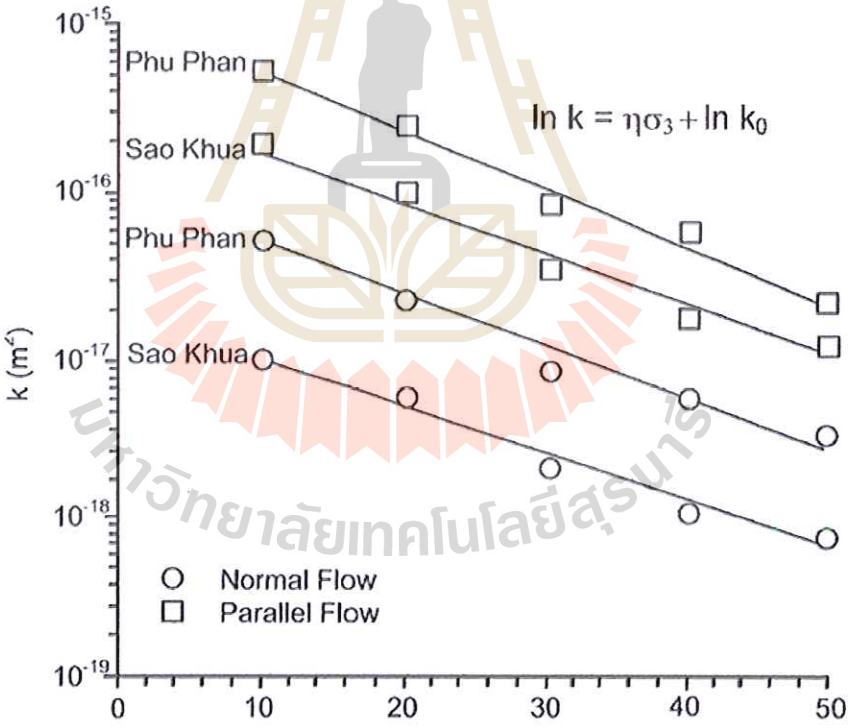

Figure 4.23 Intrinsic permeability as function of confining pressures.

Table 4.2 Summary of empirical constants.

Rock types	Flow directions	$k = k_0 \exp^{\eta\sigma_3}$		
		k_0	η	R^2
Sao Khua sandstone	Parallel	4×10^{-16}	-0.078	0.988
	Perpendicular	2×10^{-17}	-0.078	0.988
Phu Phan sandstone	Parallel	1×10^{-15}	-0.078	0.988
	Perpendicular	9×10^{-17}	-0.078	0.988

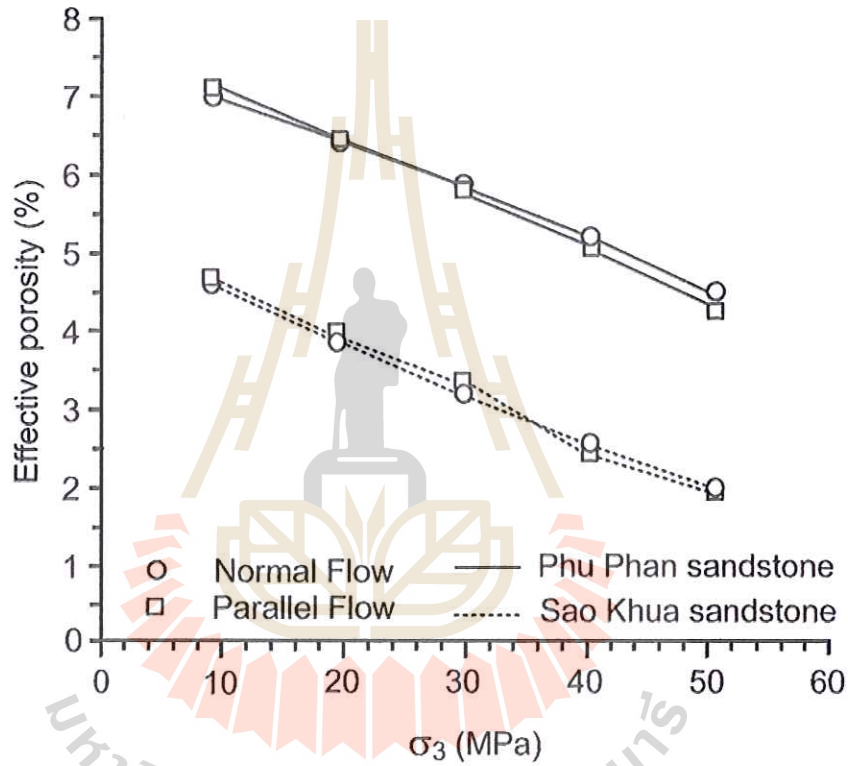

Figure 4.24 Effective porosity in directions normal and parallel to bedding plane as a function of confining pressures.

Table 4.3 Specimen diameters and lengths before and after testing for Phu Phan sandstone with parallel to bedding planes.

Confining pressures (MPa)	Pre-Test		Post-Test	
	Diameter (mm)	Length (mm)	Diameter (mm)	Length (mm)
0	53.70	77.50	53.70	77.50
10	53.70	77.50	53.58	77.18
20	53.60	83.20	53.52	82.85
30	53.70	82.70	53.54	81.35
40	53.70	82.20	53.50	82.06
50	53.60	84.00	53.48	82.73

Table 4.4 Specimen diameters and lengths before and after testing for Phu Phan sandstone with normal to bedding planes.

Confining pressures (MPa)	Pre-Test		Post-Test	
	Diameter (mm)	Length (mm)	Diameter (mm)	Length (mm)
0	53.20	83.40	53.20	83.40
10	53.30	82.40	53.28	82.26
20	53.20	83.70	53.10	83.20
30	53.70	81.60	53.52	80.88
40	53.30	82.40	53.18	81.12
50	53.20	83.40	53.00	82.04

มหาวิทยาลัยเทคโนโลยีสุรนารี

Table 4.5 Specimen diameters and lengths before and after testing for Sao Khua sandstone with parallel to bedding planes.

Confining pressures (MPa)	Pre-Test		Post-Test	
	Diameter (mm)	Length (mm)	Diameter (mm)	Length (mm)
0	53.58	83.60	53.58	83.60
10	53.70	83.60	53.50	83.45
20	53.70	79.70	53.54	79.21
30	53.64	83.34	53.28	83.03
40	53.80	83.20	53.34	82.81
50	53.58	83.60	52.92	83.08

Table 4.6 Specimen diameters and lengths before and after testing for Sao Khua sandstone with normal to bedding planes.

Confining pressures (MPa)	Pre-Test		Post-Test	
	Diameter (mm)	Length (mm)	Diameter (mm)	Length (mm)
0	54.20	81.30	54.20	81.30
10	54.10	83.60	53.96	83.44
20	53.60	84.40	53.38	84.18
30	54.24	80.40	53.88	80.12
40	53.80	81.14	53.36	80.82
50	54.20	81.30	53.74	80.78

4.6 Discussions and Conclusions

Permeability and porosity of sandstones are measured under different confining pressures ranging from 10 to 50 MPa. The results clearly indicate that the permeability of Phu Phan sandstone is higher than that of Sao Khua sandstone. Both sandstones show the anisotropic permeability. The permeability parallel to the bedding planes is about

10 times higher than that normal to the bedding planes. This permeability anisotropy tends to be independent of the confining pressure. The confining pressures within the range used here affect equally on the permeability in both flow directions. Increasing the confining pressures from 10 to 50 MPa can reduce the sandstone permeability by about one order of magnitude. The results suggest that the closure of the pore space after subjecting to high confining pressures tends to be permanent. This is evidenced from the measurements of the specimen diameters and lengths before and after testing.

มหาวิทยาลัยเทคโนโลยีสุรนารี

CHAPTER V

POTENTIAL APPLICATION

5.1 Introduction

The purpose of this chapter is to determine storativity for sandstone aquifer considering the compressibility and elasticity of the rocks. The empirical equation of porosity and permeability relationship is used to determine formation compressibility and specific storage.

5.2 Permeability-Porosity relationship under confining pressure

Fluid flow simulation in the crust requires models that reflect the relationship between permeability and depth. The exponential relationship would be suitable for describing the stress dependent permeability. The results are based on laboratory experiments (with pressures up to 50 MPa) for two different sandstones. The exponential relationship for permeability can be expressed as follows:

$$k = a \cdot \exp(b n_e) \tag{5.1}$$

where a and b are constants, and n_e is effective porosity. Figure 5.1 shows that there is a general trend of increasing permeability with increasing effective porosity and it is clear from this figure that the permeability of the two sandstone formations are controlled by the porosity. Table 5.1 shows the empirical equation and parameters use to fit the curves in Figure 5.1. The effective porosity values range from 2% to 9%, while

permeabilities between 9.10×10^{-19} to 8.2×10^{-16} m^2. For rocks of comparable porosity, a difference in permeability of up to four orders of magnitude can be observed. The permeability and porosity are in a close relationship that depends on the amount of void space in the tested material. It is widely accepted that permeability is determined by microstructure, which is, in this context, defined in terms of pore and crack structures. So, it could be supposed that with increasing porosity, the permeability should increase as well.

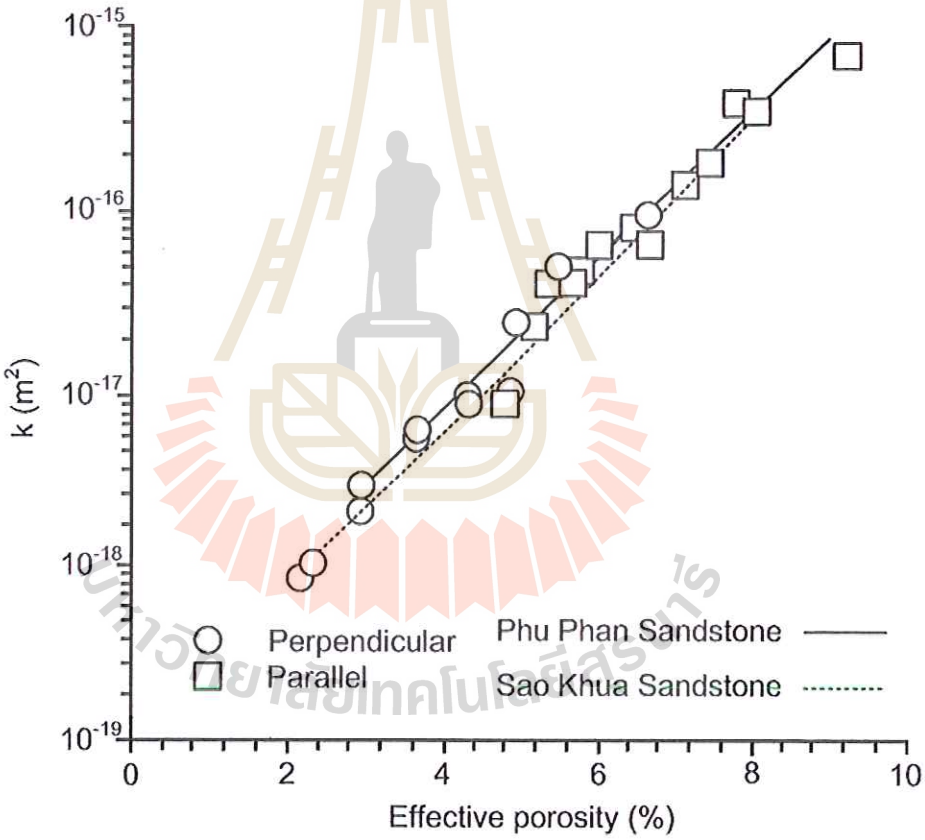

Figure 5.1 Permeability – Porosity relation empirical equation.

Table 5.1 Summary of empirical constants.

Rock types	Flow directions	$\ln k = b \cdot n_e + \ln a$		
		a	b	R^2
Sao Khua sandstone	Parallel	1×10^{-19}	0.982	0.969
	Normal			
Phu Phan sandstone	Parallel	4×10^{-19}	0.865	0.970
	Normal			

Notably, comparable values of permeability can also be associated with rocks with very different porosities. While part of this distribution may be explained by permeability anisotropy (Clavaud et al. (2008); Wright et al. (2009) and Gaunt et al. (2014)), microstructural attributes such pore geometry will contribute significantly to permeability. For instance, sandstone with single through-running crack could have very low porosity, while providing an effective fluid conduit. On the other hand, the structure consisting of many large pores connected by tortuous microcracks could be poor at transmitting fluids, despite having relatively high porosity.

5.3 Volumetric changes

The volumetric changes are calculated by dividing the volume change by the original volume of the specimen using the relation:

$$\text{Volumetric change} = V_0\text{-}V_a/\ V_0 \times 100\ (\%) \tag{5.2}$$

where V_0 is original volume (m^3) and V_a is new volume (m^3). The results in Table 5.2 show that the volumetric changes or reductions of both sandstones can be measured after they are removed from the confining chamber. It is found that the specimen volume reduces as increasing the confining pressure.

Table 5.2 Volumetric change of specimens under each confinement for Phu Phan and Sao Khua sandstone.

Confining pressures (σ_3) (MPa)	Dry density (g/cc)		Volumetric change (%)	
	Sao Khua sandstone	Phu Phan sandstone	Sao Khua sandstone	Phu Phan sandstone
0	2.365	2.409	0	0
10	2.387	2.421	0.950	0.520
20	2.394	2.437	1.220	1.170
30	2.406	2.446	1.730	1.530
40	2.417	2.461	2.220	2.160
50	2.423	2.468	2.470	2.470

This suggests that permanent closure of the pore spaces has occurred after the specimens have been subjected to the confining pressures. The greater confinement is applied, the more permanent pores closure is obtained (Figure 5.2).

5.4 Formation compressibility

The compressibility is relative volume change of fluid or solid in a response to pressure change that can relate into a reservoir. The reduction of volume in relation to pressure is called volume compressibility (c_f) or formation compressibility (Dandekar,2013) it can be expressed as follows:

$$c_f = \frac{1}{K} \tag{5.3}$$

where K is bulk modulus (GPa), The bulk modulus is another elastic constant that reflects the resistance of the material to an overall gain or loss of volume in conditions of hydrostatic stress and it can be expressed as follows in:

$$K = \frac{\sigma_3}{\Delta} \tag{5.4}$$

where σ_3 is confining pressure (MPa) and Δ is volumetric change (%). For an ideal elastic material, the elastic parameters obtained from hydrostatic compression are equivalent. However, in rocks the presence of porosity causes the elastic parameters obtained from the tests to be different. All the elastic parameters of both sandstone formation increase with increasing confining pressure (Table 5.3). On the other hand, the formation compressibility decreases with increasing confining pressure.

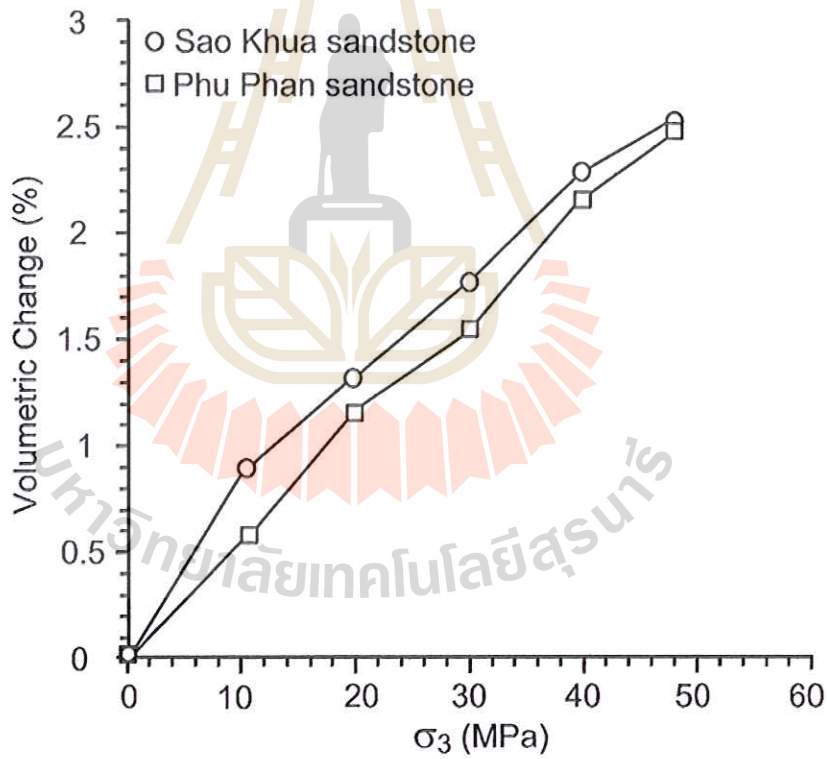

Figure 5.2 Volumetric change as a function of confining pressure.

5.5 Storativity of sandstone

Specific storage (S_s) is the volume of water that a unit volume of aquifer releases from storage under a unit decline in hydraulic head (Freeze and Cherry, 1979). Specific storage is related to the compressibility of water and aquifer. It can be determined by:

$$S_s = \rho_w g\,(c_f + n_e\beta) \tag{5.5}$$

where ρ_w is mass density of water (1,000 kg/m^3), g is gravitational acceleration (9.8 m/sec^2), c_f is formation compressibility (Pa^{-1}) (Table 5.4), β is compressibility of water (4.4×10^{-10} Pa^{-1}), and n_e is average effective porosity.

The storativity (S) of confined aquifer is defined as the volume of water released from storage per unit surface area of the aquifer. In a confined aquifer, storativity can be calculated by:

$$S = S_s t \tag{5.6}$$

Table 5.3 Constants used to calculate sandstone formation compressibility.

σ_3 (MPa)	Δ (%)		K (GPa)		c_f (GPa^{-1})	
	Sao Khua	**Phu Phan**	**Sao Khua**	**Phu Phan**	**Sao Khua**	**Phu Phan**
10	0.95	0.52	0.011	0.019	95.00	54.00
20	1.22	1.03	0.016	0.020	61.00	51.50
30	1.73	1.53	0.017	0.020	57.70	51.00
40	2.22	2.03	0.018	0.020	55.50	50.75
50	2.47	2.47	0.020	0.020	49.40	49.40

มหาวิทยาลัยเทคโนโลยีสุรนารี

Table 5.4 Summary of constant to calculated storativity of sandstone.

σ_3 (MPa)	n_e		$S_s \times 10^{-4}$ (m^{-1})		S	
	Sao Khua sandstone	**Phu Phan sandstone**	**Sao Khua sandstone**	**Phu Phan sandstone**	**Sao Khua sandstone**	**Phu Phan sandstone**
10	4.59	7.01	9.52	5.60	0.095	0.084
20	3.22	6.47	6.12	5.33	0.061	0.080
30	3.82	5.86	5.83	5.26	0.058	0.079
40	2.58	5.22	5.56	5.20	0.056	0.078
50	2.00	4.50	4.93	5.04	0.049	0.076

where S_s is specific storage (m^{-1}) and t is aquifer thickness (m). In this study n_e (effective porosity) is taken as 6.20% for Phu Phan sandstone, and 3.58% for Sao Khua sandstone. Table 5.4 shows the storativity of sandstone calculated from specific storage that the parameter is calculated by elastic properties from laboratory testing. The storativity increases with porosity and decreases with confining pressure (depths). The effective porosity for Phu Phan sandstone, is greater than that of Sao Khua sandstone. It is possible that the storativity increases with porosity and decrease with depths.

5.6 Discussions and Conclusions

The permeability and porosity are used to develop exponential relationship describing the stress dependent permeability-porosity. There is a general trend of increasing permeability with increasing effective porosity. The volumetric changes of the sandstone specimens have been measured after they are removed from the confining chamber. It is found that the specimen volume reduces as increasing the confining pressure. This suggests that permanent closure of the pore spaces has occurred after the specimens have been subjected to the confining pressures. The greater confinement is

applied, the more permanent pores closure is obtained. However, this effect shows very low or no influence on the volumetric change at greater confining pressures.

The bulk modulus is used to calculate formation compressibility to determine the storativity under various confining pressure (depths). The results show that the storativity increase when the effective porosity increase and tend to be sensitive with depths.

มหาวิทยาลัยเทคโนโลยีสุรนารี

CHAPTER VI

DISCUSSIONS AND CONCLUSIONS

6.1 Discussions

This section discusses the key issues relevant to the reliability of the test schemes and the adequacies of the test results. Comparisons of the results and findings from this study with those obtained elsewhere under similar test conditions have also been made.

The hydraulic properties for the sandstone specimens prepared from different formations can give an understanding of which pore characteristics, flow direction and confining pressure have an impact on the hydraulic properties.

Permeability and porosity depend on pores in the specimens. There are two discerned typologies of pores in rocks; closed and open pores. Closed pores are completely isolated from the external surface, not allowing the access of external fluids in either the liquid or gaseous phase. Open pores are connected to the external surface and are therefore accessible to fluids, depending on the pore characteristics and the nature of fluid. The percentage of interconnected pores within the rock is known as effective porosity. Effective porosity excludes isolated pores and pore volume occupied by water adsorbed on clay minerals or other grains. As a result, only effective porosity can influence permeability because only open pores are interconnected and allow leaking water through which agrees with the results obtained by Šperl Jan and Jiřina Trčková (2008) and Xuetao and Su Huang (2017). The primary porosity of rocks

mainly depends upon the shape (sphericity and roundness), sorting, and packing pattern of sediment particles. Angularity of sediment may increase or decrease porosity, depending if the particles openings are packed together like pieces of a mosaic. It can be proved that the porosity is always related with the size and sorting of rock particles. In general, well-sorted sediments are more porous and have higher porosity than poorly sorted ones because small grains take up space between large grains as described by Xuetao and Su Huang (2017).

The changes in porosity due to deformation are controlled by alterations in grain size and distributions and by the production of microstructures which can modify pore connectivity. With decreasing in porosity can occur due to grain size rearrangement, confining pressure and cementation. The porosity decreases as the confining pressure increases due to pore space becomes to be compressed and grains increasingly compact. However, dissolved minerals, such as quartz, may also form new crystals in pore, which leads to a further decrease in porosity as described by Xuetao and Su Huang (2017).

The anisotropic of rock permeability can be attributed to the arrangement direction of sand grains. In the deposition process, the long axis of sand is mainly parallel to the flow direction. The arrangement orientation of the rock matrix and the filling mode are closely linked to the direction of permeability. The anisotropy of rock permeability is measured in two directions (parallel and normal with bedding planes of specimens). The permeability increases significantly in the parallel to the bedding planes and, is higher than that normal to the bedding planes which agrees with Renner (2000) and Chen (2009). The significant variables affecting the permeability of rock are porosity, mineral compositions and confining pressures which agrees with the results obtained by Wannakao (2014). The permeability tends to decrease as the

confining pressure increases which agrees with the results obtained by Wannakao (2010) and Sukplum (2012). The effect of confining pressure reduces the overall magnitude of permeability as described by David (1994).

6.2 Conclusions

All objectives and requirements of this study have been met. The results of the laboratory testing and analyses can be concluded as follows.

The flow rates of Phu Phan and Sao Khua sandstones are measured as a function of time until the inflow and outflow rates are equal. This is to ensure that the specimens are under saturated condition, and that the mass balance flow rates are reached. The results indicate that the outflow rate increases with times and decreases with increasing confining pressures. The time at which the inflow and outflow rates are balanced increases with increasing confining pressures. For both sandstone types, the flow rates normal to the bedding plane are lower than those parallel to the bedding plane. The Phu Phan sandstone gives the flow rate higher than that of Sao Khua sandstone for both normal and parallel to the bedding planes. This is probably controlled by the porosity and pore space arrangement of the specimens.

The effective porosity of Phu Phan sandstone is higher than that of Sao Khua sandstone, particularly under high confining pressures. They range from 4.5% to 7.3% for Phu Phan sandstone and 1.9% to 4.3% for Sao Khua sandstone.

The permeability of sandstone is measured under different confining pressures ranging from 10 to 50 MPa. The results clearly indicate that the permeability of Phu Phan sandstone is higher than that of Sao Khua sandstone. Both sandstones show the anisotropic permeability. The permeability parallel to the bedding planes is about 10

times higher than that normal to the bedding planes. This permeability anisotropy tends to be independent of the confining pressure. The confining pressures within the range used here affect equally on the permeability in both flow directions. Increasing the confining pressures from 10 to 50 MPa can reduce the sandstone permeability by about one order of magnitude.

The permeability and porosity are used to develop exponential relationship describing the stress dependent permeability-porosity. There is a general trend of increasing permeability with increasing effective porosity. The volumetric changes of the sandstone specimens have been measured after they are removed from the confining chamber. It is found that the specimen volume reduces as increasing the confining pressure. This suggests that permanent closure of the pore spaces has occurred after the specimens have been subjected to the confining pressures. The greater confinement is applied, the more permanent pores closure is obtained. However, this effect shows very low or no influence on the volumetric change at greater confining pressures.

The bulk modulus is used to calculate formation compressibility to determine the storativity under various confining pressure (depths). The results show that the storativity increase when the effective porosity increase and tend to be sensitive with depths.

6.3 Recommendations for future studies

Recognizing that the numbers of the specimens and the test parameters used here are limited, more testing and measurements are recommended, as follows:

(1) More testing is required on a variety of rock types with different confining pressures.

(2) More testing is required on fracture in the same rocks tested have for constant head flow testing with different confining pressures.

(3) Increasing the number of the test specimens would statistically enhance the reliability of the test results.

มหาวิทยาลัยเทคโนโลยีสุรนารี

REFERENCES

ASTM C830-00. Standard Test Methods for Apparent Porosity, Liquid Absorption, Apparent Specific Gravity, and Bulk Density of Refractory Shapes by Vacuum Pressure. ASTM International, West Conshohocken, P.A., vol.15.01

ASTM D2434-68. Standard Test Method for Permeability of Granular Soils (Constant head). ASTM International, West Conshohocken, P.A., vol. 04.08.

ASTM D4543-08. Standard Practices for Preparing Rock Core as Cylindrical Test Specimens and Verifying Conformance to Dimensional and Shape Tolerances. ASTM International, West Conshohocken, P.A., vol. 04.08.

Baud, P., Zhu, W., and Wong, T. F. (2000). Failure mode and weakening effect of water on sandstone. **Journal of Geophysical Research: Solid Earth**. 105(B7): 16371-16389.

Bloomfield, J.P. and Williams, A.T. (1995). An empirical liquid permeability gas permeability correlation for use in aquiferproperties studies. **Quarterly Journal of Engineering Geology and Hydrology.** 2802: 143-150.

Brace, W. F., Walsh, J.B., and Francos, W. T. (1968). Permeability of granite under high pressure. **Journal of Geophysical Research**. 73(6): 2225-2236.

Bjorlykke, K., Jahren, J., Mondol, N. H., Marcussen, O., Croize, D., Peltonen, C. and Thyberg, B. (2008). PS Sediment Compaction and Rock Properties. Search and Discovery Article 50192. **Poster presentation at AAPG International Conference and Exhibition**. Cape Town, South Africa, Oct 26-29.

Charukalas, B. (1975). Hydraulic conductivity of sandstone under difference confining pressure. **M.S. thesis.** New Mexico Institute of Mining and Technology, Socorro, New Mexico.

Chen, T. M. N., Zhu, W., Wong, T. F., and Song, S. R. (2009). Laboratory characterization of permeability and its anisotropy of Chelungpu Fault rocks. **Pure and Applied Geophysics**. 166: 1011–1036.

Clavaud, J. B., Maineult, A., Zamora, M., Rasolofosaon, P., and Schlitter, C. (2008). Permeability anisotropy and its relations with porous medium structure. **Journal of Geophysical Research**. Solid Earth, 113(B1).

Dandekar, A. Y. (2013). **Petroleum reservoir rock and fluid properties**. CRC press, London.

David, C., Wong, T., Zhu, W. and Zhang, J. (1994). Laboratory measurement of compaction-induced permeability change in porous rocks: implications for the generation and maintenance of pore pressure excess in the crust. **Pure and Applied Geophysics**. 143: 425- 456.

Davies, J. P. and Davies, D. K. (1999). Stress-dependent permeability: characterization and modeling. In **SPE Annual Technical Conference and Exhibition.** Society of Petroleum Engineers. Houston, Texas.

Davies, J. P. and Holditch, S. A. (1998). Stress dependent permeability in low permeability gas reservoirs: Travis Peak Formation, East Texas. In **SPE Rocky Mountain Regional/Low-Permeability Reservoirs Symposium.** Society of Petroleum Engineers. Denver, Colorado.

Department of mineral resources. (1992). Lexicon of stratigraphic names of Thailand. **Department of Mineral Resources**. Bangkok, Thailand, 1–129.

Dickinson, W. R. and Suczek, C. A. (1979). Plate tectonics and sandstone composition **AAPG Bulletin**. 63(12): 2164-2182.

Dong, J. J., Hsu, J. Y., Wu, W. J., Shimamoto, T., Hung, J. H., Yeh, E. C., Wu, Y.H. and Sone, H. (2010). Stress-dependence of the permeability and porosity of sandstone and shale from TCDP Hole-A. **International Journal of Rock Mechanics and Mining Sciences**. 47(7): 1141-1157.

Freeze, R. A., and Cherry, J.A. (1979). **Groundwater**. Englewood Cliffs: Prentice Hall,USA, pp.604.

Gaunt, H.E., Sammonds, P.R., Meredith, P.G., Smith, R. and Pallister, J.S. (2014). Pathways for degassing during the lava dome eruption of Mount St. Helens. **Geology**. 42 (11): 947–950.

Ghabezloo, S., Sulem, J., Guedon, S., and Martineau, F. (2009). Effective stress law for the permeability of a limestone. **International Journal of Rock Mechanics and Mining Sciences**. 46(2): 297-306.

Heiland, J. (2003). Permeability of triaxially compressed sandstone: Influence of deformation and strain-rate on permeability. **Pure and Applied Geophysics**. 160: 889-908.

Huiyuan, B., Fei, W., Yonghao, Z., Chaowei, D., and Gang, C. (2016). Pressure sensitivity research on porosity, permeability and acoustic slowness in tight sandstone reservoir. **Electronic Journal of Geotechnical Engineering**. 21(24): 7719-7727.

Indraratna, B. and Ranjith, P. (2001). **Hydromechanical aspects and unsaturated flow in jointed rock**. Lisse: AA Balkema publishers, Netherlands.

มหาวิทยาลัยเทคโนโลยีสุรนารี

Jennings, J. B., Carroll, H. B., and Raible, C. J. (1981). The relationship of permeability to confining pressure in low permeability rock. In **SPE Low Permeability Gas Reservoirs Symposium**. Society of Petroleum Engineers. Denver, Colorado.

Jones, S.C. and Marathon, O.C. (1988). Two-point determination of permeability and PV vs. Net Confining Stress. **SPE Formation Evaluation**. 3(1): 235-241.

LaMoreaux, P. E., Charaljavanaphet, J., Jalichan, N., Chiengmai, P. P. N., Bunnag, D., Thavisri, A. and Rakprathum, C. (1958). Reconnaissance of the geology and ground water of the Khorat Plateau, Thailand. **U.S. Geological Survey Water-Supply Paper 1429**. 62 p.

Lewis, J.J.M. (1988). Outcrop-derived quantitative models of permeability heterogeneity for genetically different sand bodies. **SPE Annual Technical Conference and Exhibition of the Society of Petroleum Engineers**. Houston, Texas, Oct 2-5, 449-463.

Luffel, D. L., Howard, W. E., and Hunt, E. R. (1991). Travis Peak core permeability and porosity relationships at reservoir stress. **SPE Formation Evaluation**. 6(03): 310-318.

Meesook, A., Suteethorn, V., Chaodumrong, P., Teerarungsigul, N., Sarsud, A. and Wongprayoon, T. (2002). Mesozoic rocks of Thailand: A summary. In **Proceedings of the Symposium on Geology of Thailand** (pp. 22-94). Department of Mineral Resources, August 26-28, Bangkok, Thailand.

Mohiuddin, M. A., Korvin, G., Abdulraheem, A., Awal, M. R., Khan, K., Khan, M. S., and Hassan, H. M. (2000). Stress-dependent porosity and permeability of a suite of samples from Saudi Arabian sandstone and limestone reservoirs. In **Symposium of Core Analysts**. Abu Dhabi, UAE.

Peng, S. P., Meng, Z. P., Wang, H., Ma, C. L., and Pan, J. N. (2003). Testing study on pore ratio and permeability of sandstone under different confining pressures. **Chinese Journal of Rock Mechanics and Engineering.** 22(5): 742-746.

Racey, A. and Goodall, J. G. S. (2009). Palynology and stratigraphy of the Mesozoic Khorat Group red bed sequences from Thailand. **Geological Society**. London, Special Publications, 315(1): 69-83.

Racey, A., Love, M. A., Canham, A.C., Goodall, J. G. S., Polachan, S., and Jones, P. D. (1996). Stratigraphy and reservoir potential of the Mesozoic Khorat Group, NE Thailand. Part I: Stratigraphy and sedimentary evolution. **Journal of Petroleum Geology**. 5-40.

Renner, J., Hettkamp, T., and Rummel, F. (2000). Rock mechanical characterization of an argillaceous host rock of a potential radioactive waste repository. **Rock mechanics and rock engineering**. 33(3): 153-178.

Sattayarak, N. (1983). Review of the continental Mesozoic stratigraphy of Thailand. In **Proceeding and Workshop on Stratigraphic Correlation of Thailand and Malaysia** (Vol.1, pp.127-140). September, Bangkok.

Sattayarak, N. and Srigulawong, S. (2008). The Western Khorat Plateau Geological Field Trip. **Journal of the Geological Society of Thailand**. 1: 1–40.

Sharp Jr, J. M. and Domenico, P. A. (1976). Energy transport in thick sequences of compacting sediment. **Geological Society of America Bulletin**. 87(3): 390-400.

Shijia, M. (2017). Permeability evolution of chalk under different stress states. **M.S. thesis.** Faculty of Science and Technology, University of Stavanger, Norway.

Songsawad, R. and Chutakositkanon, V. (2009). Lithostratigraphy of part of Sao Khua Formation at Khao Phang Hoei Area, Amphoe Thepsatit, Changwat Chaiyaphum. **Bulletin of Earth Sciences of Thailand (BEST).** 2(1): 81-83.

Sperl, J. and Trckova, J. (2008). Permeability and porosity of rocks and their relationship based on laboratory testing. **International Journal of Acta Geodynamica et Geromaterialia (AGG).** 5(1): 41-48.

Sukplum, W. (2012). Experimental assessment of the sandstone anisotropic permeability, the Nam Phong formation, Loei-Phetchabun fold belt by gas and water flowing measurements under confining pressures. **M.S. thesis**. Khon Kaen University.

Sukplum, W., Wannakao, L., Yongmee, W., and Trakoolngam, K. (2013). Experimental assessment of the anisotropic permeability of sandstone, Nam Phong formation Loei-Phetchabun fold belt by gas flowing under confining pressures. In **Proceedings of the Fourth Thailand symposium on Rock Mechanics.** Im Poo Hill Resort, Nakhon Ratchasima.

Vairogs, J., Hearn, C.L., Dareing, D.W., and Rhoades, V.W. (1971). Effect of rock stress on gas production from low-permeability reservoirs. **Journal of Petroleum Technology.** pp. 1161-1167.

Wang, H. L., Xu, W. Y., Zuo, J., Shao, J., and Jia, C. (2015). Evolution law of the permeability and porosity for low-permeability rock based on gas permeability test. **Journal of Hydraulic Engineering**. 46(2): 208-216.

Wannakao, L., Sukplum, W., Yongmee, W., Wannakao, P., and Trakoolngam, K., (2014). Correlation between Gas and Water Permeabilities of the Nam Phong

Formation Sandstones and their Factors Affecting. In **ISRM International Symposium-8th Asian Rock Mechanics Symposium**. Sapporo, Japan.

Wannakao, L., Wannakao P., and Yungme W., (2010). The Use of Ultrasonic in Evaluating Engineering Properties: Phra Wihan, Phu Phan, Nam Phong Sandstones and Permian Limestone. **Research Report**. no.1, Khon Kaen, Department of Geotechnology, Faculty of Technology, Khon Kaen Unversity.

Ward, D. E. and Bunnag, D. (1964). Stratigraphy of the Mesozoic Khorat Group in Northeastern Thailand. **Report of investigation no.6**, Bangkok: Department of Mineral Resources.

Weber, K.J. (1982). Influence of common sedimentary structures on fluid flow in reservoir models. **Journal of Petroleum Technology**. 34: 665-672.

Whitaker, S. (1986). Flow in porous media I: A theoretical derivation of Darcy's law. **Transport in porous media.** 1(1): 3-25.

Wilson, M.D. and Stanton, P.T. (1994). Diagenetic mechanism of porosity and permeability reduction and enhancement: Reservoir Quality Assessment and Prediction in Clastic Rocks, **Society for Sedimentary Geology, Short Course 30.** 59-118.

Wong, T. F., David, C., and Zhu, W. (1997). The transition from brittle faulting to cataclastic flow in porous sandstones: Mechanical deformation. **Journal of Geophysical Research: Solid Earth**. 102(B2): 3009-3025.

Wright, H. M., Cashman, K. V., Gottesfeld, E. H., and Roberts, J. J. (2009). Pore structure of volcanic clasts: measurements of permeability and electrical conductivity. **Earth and Planetary Science Letters**. 280(1-4): 93-104.

มหาวิทยาลัยเทคโนโลยีสุรนารี

Xuetao, Hu. and Huang, Su. (2017). **Physical Properties of Reservoir Rocks**. In Physics of Petroleum Reservoirs. Springer, Berlin, Heidelberg.

Yu, J., Chen, S. J., Chen, X., Zhang, Y. Z., and Cai, Y. Y. (2016). Experimental investigation on mechanical properties and permeability evolution of red sandstone after heat treatments. **Journal of Zhejiang University SCIENCE-A**. 16(9): 749-759.

Zhag, M., Takeda, M., Esaki, T., Takahashi, M., and Endo, H. (2000). Effect of confining pressure on gas and water permeabilities of rocks. **MRS Online Proceedings Library (OPL).** 663: 851.

Zhang, R., Ning, Z., Yang, F., Zhao, H., and Wang, Q. (2016). A laboratory study of the porosity-permeability relationships of shale and sandstone under effective stress. **International Journal of Rock Mechanics and Mining Sciences.** 81: 19-27.

Zhijiao, Z.E.N.G., Xiaochun, L. I., Lu, S.H.I., Bing, B.A.I., Zhiming, F.A.N.G., and Ying, W.N.G. (2014). Experimental study of the laws between the effective confining pressure and mudstone permeability. **Energy Procedia**. 63: 5654-5663.

Zisser, N. and Nover, G. (2009). Anisotropy of permeability and complex resistivity of tight sandstones subjected to hydrostatic pressure. **Journal of Applied Geophysics.** 68(3): 356-370.

มหาวิทยาลัยเทคโนโลยีสุรนารี

BIOGRAPHY

Miss Sawarin Champanoi was born on March 29, 1994 in Lopburi, Thailand. She received her Bachelor's Degree in Engineering (Geotechnology) from Suranaree University of Technology in 2016. For her post-graduate, she continued to study with a Master's degree in the Geological Engineering Program, Institute of Engineering, Suranaree university of Technology. During graduation, 2016-2018, she was a part time worker in position of research assistant at the Geomechanics Research Unit, Institute of Engineering, Suranaree University of Technology.

มหาวิทยาลัยเทคโนโลยีสุรนารี